Department of Electrical and Computer Systems Engineering

Technical Report
MECSE-24-2006

40Gb/s Amplitude and Phase Modulation Optical Fibre Transmission Systems

L.N. Binh, H.S. Tiong and T.L. Huynh

MONASH UNIVERSITY

40Gb/s amplitude and phase modulation optical fibre transmission systems: PART I: Simulink modeling

L.N. Binh, H.S. Tiong and T.L. Huynh

Laboratory for Optical Communications and Applied Photonics, Centre for Telecommunications and Information Engineering, Department of Electrical and Computer Systems Engineering, Monash University, Wellington Rd., Clayton 3168, Australia. le,nguyen.binh@eng.monash.edu.au

SUMMARY

Advanced optical fibre communications have been attracting tremendous interests in recent years due to urgent demands on the upgrading of the fibre backbone transmission systems and networks. In these modern optical transmission systems modulation techniques employing amplitude, phase and/or frequency shift keying modulation schemes are considered to be the keys for reducing the signal and carrier spectral properties. Together with these schemes the formats of the pulse sequence such as return–to-zero (RZ), non-return-to-zero (NRZ), carrier suppressed RZ or duo-binary or bi-phase shaping of the pulse sequence are considered to optimize the transmission energy contents o the transmitted sequence and hence enhancement the total transmission distance without violating the nonlinear/linear limit of the transmission or dispersion compensating fibres.

This report is the PART I of the series of technical investigation of the amplitude shift keying and phase shift keying modulation formats in association with the RZ, NRZ and CSRZ and duobinary formats so that the simulated results can be corroborated with those obtained in experimental demonstration that are the subjects of the PART II of the series. The modeling platform is based on the MATLAB Simulink as this mathematical and graphical modeling package offer sufficient all signal representation and processing blocksets that allow the generation, modulation and processing of lightwaves and signals schemes at optical frequency in the passband and baseband domains. Furthermore it offers a range of equipment that could be employed to inspect signals in temporal and spectral domain to study the impacts of the modulation spectra on the transmitted data sequence.

Models have been developed for ASK and DPSK for all formats and their transmission, especially the dispersion tolerance, over standard SMF fibers are demonstrated. Furthermore duo-binary modulation scheme with alternating phase property is also demonstrated.

The developed models have been proven effective in the transmission and receiving by interferometric delay schemes for differential detection and recovery of the pre-coded sequence. The optical modulation employing external modulators such as the electro-absorption (EA) and electro-optic (EO) is very important for modulation schemes using both amplitude and phase. These are exploited in our study with the EA and LiNbO$_3$ type modulators. We note that the models representing photonic components such as the modulators, inteferometric delay balanced receiver, are operating in the photonic domain. That is the interaction between guided optical waves and traveling wave electrical signals represent exactly the real electro-optic operation. No mathematical representation is used. This contrasts the modeling of several packages developed for optical communications systems in which the mathematical languages have been used. The Simulink models are thus described wherever appropriate to prove these findings.

_____ **2**

TABLE OF FIGURES

_____ **4**

1   INTRODUCTORY REMARKS

Owing to tremendous growing demand on high capacity transmission over Internet, high data rate of 40 Gb/s per channel has appeared to be an attractive feature in the next generation of light wave communications system. Under the current 10 Gb/s DWDM optical system, overlaying 40 Gb/s on the existing network can be considered to be the most cost effective method for upgrading purpose. However, there are a number of technical difficulties confronted by communications engineers involving interoperability that requires 40 Gb/s line system to have signal optical bandwidth, tolerance to chromatic dispersion, resistance to non linear crosstalk, susceptibility to accumulated noise over multi-span of optical amplifier to be similar to 10 Gb/s system.

In view of this, advanced modulation formats have been demonstrated as an effective scheme to overcome 40 Gb/s system impairments. Differential Phase Shift Keying (DPSK) modulation format has attracted extensive studies due to its benefit over conventional On-Off Keying(OOK)[1] or amplitude shift keying (ASK) signaling format, including 3-dB lower optical signal-to-noise ratio (OSNR) [1] at a given bit-error-rate (BER), more robust to narrow band optical filtering, more resilient to some non linear effects such as cross phase modulation and self phase modulation. Moreover, spectral efficiencies can be improved by using multi-level signaling. On top of that, coherent detection is not critical as DPSK detection requires comparison of two consecutive pulses; hence the source coherence is required only over one bit period.

Nevertheless, DPSK format involves rapid phase change causing intensity ripples due to chromatic dispersion that induce pattern dependent SPM-GVD (group velocity dispersion) effect.[2] Therefore, return-to-zero (RZ) pulse can be employed in conjunction with DPSK to generate more tolerance to the data pattern dependent SPM-GVD effect. In addition, RZ improves dispersion tolerance and non linear effects particularly in long haul network at high data rate. Specific RZ format like carrier-suppressed RZ (CSRZ) helps to reduce the inherent larger spectral bandwidth.

At 40 Gb/s, generation of RZ pulse is not feasible as it is at 10 Gb/s due to the large bandwidth requirement. Thus, 40 Gb/s RZ signals are produced optically in "pulse carver" by driving the modulator with 20 GHz RF signal. With the remarkable advancement in external modular, especially Mach-Zehnder interferometic modulator (MZIM), this is easily achieved by utilizing microwave optical transfer characteristic of MZIM.

In this report, in order to investigate the viability of RZ-DPSK modulation formats for the next generation of lightwave communication system, especially for ultra-high capacity and ultra-long haul link, simulations have been conducted extensively based on MATLAB[TM] Simulink platform. A user friendly environment SIMULINK provides fast design and modeling tools to simulate components and essential devices such as MZIM. System performances, optical signal bandwidth, eye diagram, error probabilities can be evaluated instantaneously by changing design parameters. In high cost and expensive long haul optical transmission system, these simulation results are important for communication engineers to design network configurations prior to experiment and installation.

---

[1] **T**he term Amplitude Shift Keying (ASK) is preferred rather than OOK as it reflects the quasi-coherence of the detection scheme in which the amplitude and phase of the carriers do contribute to the sensitivity of the receiving system.

This report is organized as follows: In the next section, a general optical communication system comprised of essential photonic components in single channel and multichannel structure is described. In Section 3, the basic principles of components in photonic transmitter such as laser source and optical modulators are discussed. Section 4 gives principal propagation constant and its second and third order parameters that would severely distort the carrier modulated data sequence. Signal propagation model using Non linear Schrödinger Equation (NLSE) by accommodating fiber characteristics and solutions to NLSE are illustrated in Section 5.

The principles of generation by using Mach Zehnder Interferometric structures based on biasing voltage and voltage swing of the modulating signals and characteristics such as signal spectra of different modulation formats are depicted in Section 6. The Receiver structures and working principles based on single ended and balanced detection are explained in Section 7.

In Section 8, modeling design process of optical source, MZIM, fiber propagation, receiver and bit error rate evaluation are described. Particularly, the results of RZ-DPSK are illustrated to prove the interconnection and working of each module. In Section 9, system performances such as dispersion tolerance of different modulation format, advantage of balanced detection over single ended detection, penalty of mismatch in MZDI are presented. Analysis is included to discuss strength and limitations of the developed models.

Finally, concluding remarks about novelties of the developed models and future works on improving the simulator are given.

2   ADVANCED OPTICAL COMMUNICATION SYSTEM

.
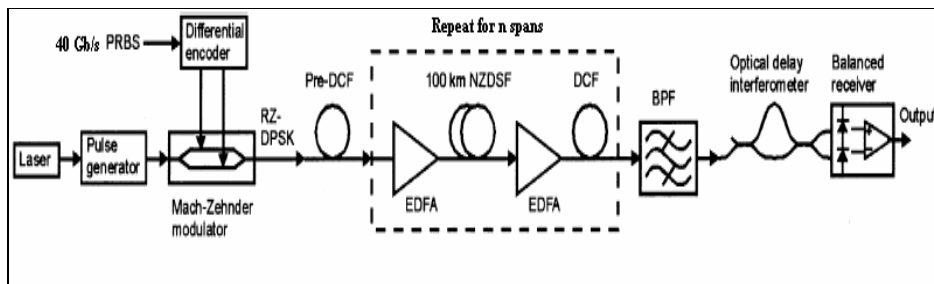
Figure 2- 1 A single channel point-to-point link of RZ-DPSK transmission system (extracted from [3])

The transmitter consists of a modulator which is responsible to convert data in electrical domain to optical domain either directly or externally using electro-optic or electro absorption modulator. The modulated optical signal is then transmitted through a single mode optical fiber using compensating fibers. In long haul link, propagation loss is considered to be significant and requires optical amplifier to boost optical signal power at the span of 80 to 120 km at regeneration point. At the receiver, the optical signal is detected using typical PIN photodiode or avalanche photodiode with gain equalization, chromatic compensation. The signal is decoded and regenerated in electrical domain for user output.

The next level of complexity in optical transmission system involved addition of multiple wavelength of light on a single fiber to make full use utilizing costly bandwidth efficiently. Each channel consists of a wavelength of light, which is a distinct "color" that can be combined with multiplexer for transmission and separated at receiver with demultiplexer. This technique is called wavelength-division-multiplexing (WDM) and a typical WDM system is illustrated in Figure 2- 2 .

As exponential growing internet traffic puts higher data rate on extreme high demand, DWDM system is realized by multiplexing more channels within a band window with approximately 100 GHz spacing. With the advent of erbium-doped fiber amplifiers (EDFA), DWDM is made practical and economical by allowing multitude of wavelengths in the fiber to be boosted simultaneously.
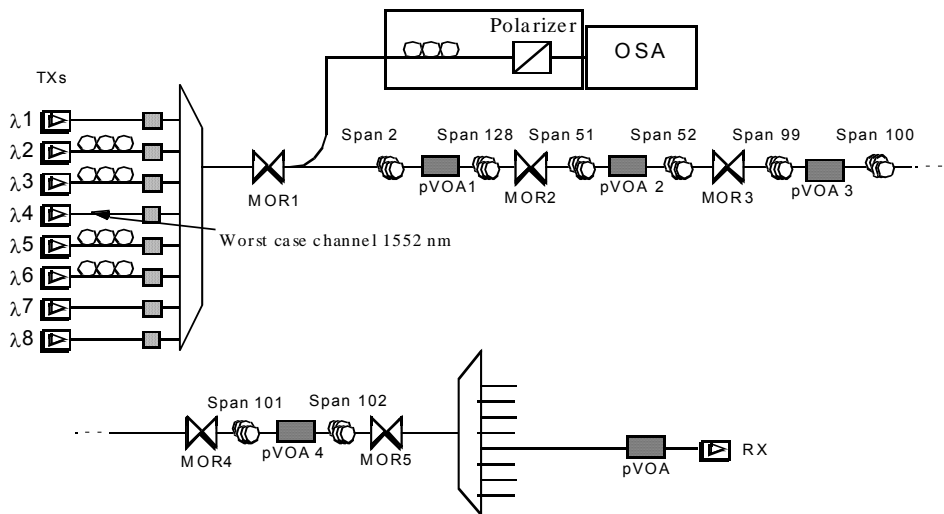
Figure 2- 2 Typical long haul DWDM multi-spans optical fibre transmission system, MOR = mid-span optical regenerator, VOA = variable optical attenuator, OSA = opticl spectrum analyzer, Tx = transmitter, Rx = receiver

3   PHOTONIC TRANSMISSION SUB-SYSTEMS

3.1   Optical Source

In this report, we simulate only distributed feedback laser (DFB) due to its superior performance and characteristics in long haul communication link. DFB lasers have narrow line widths typically about 100 MHz. Line width is range of wavelengths to describe how coherent of real sources produce radiation. Narrower line width is attributed to less sensitivity to temperature variation than other laser sources. The wavelength shifts are under 0.1nm/^{o}C owing to stabilization from grating. For this reason, in this report, DFB lasers can be characterized using a single frequency sine wave function provided in Matlab SIMULINK which we assume nearly monochromatic.

3.2   Optical Modulators

It is important to note that laser diode presents problems to optical modulation because it has a threshold current. Since threshold current is age and temperature dependent, degradation will result in L-I curve. (L-I curve is a representation of relationship between output light signal and direct current of laser diode)[4, 5] Generally external modulators consist of electro absorption modulators and electro-optic modulators. The common operating principle is based on electro optic effect (change of refractive index in material is proportional to the applied electric field). This is extremely useful in high speed operation because refractive index changes quickly with respect to the applied electric field.

Electro absorption modulators are monolithic semiconductor planar waveguide. They operate on either Fraz-Keldysh effect (FKE) or quantum stark effect by forming multiple quantum wells that consist of multiple p-type and n-type layers. The advantages of using these modulators are chirp relaxation (even though there is some inherent chirp), high input impedance and monolithically integrated on the same semiconductor chip with the laser diode.[5] This offers greater advantage over electro optic (EO) modulators since insertion loss can be reduced. The modulators are diodes that operate in reverse bias. When there is no bias voltage, electro absorption modulators are transparent to incoming optical signal. On the other hand, the applied voltage can generate a photocurrent that increases waveguide attenuation and signal losses. In other words, output power from electro absorption modulators are the highest with no applied bias voltage and decrease as the bias voltage increase as shown in Figure 3- 1 (b). It is noted that the optical modulation index of EA modulators does not reach unity so there are some residual optical power level and this may cause an increase in the zero level and hence lower the Q-facto or the BER of the transmission syste. For this reason the MZIM is preferred which will be described in the next section.

(a)   (b)
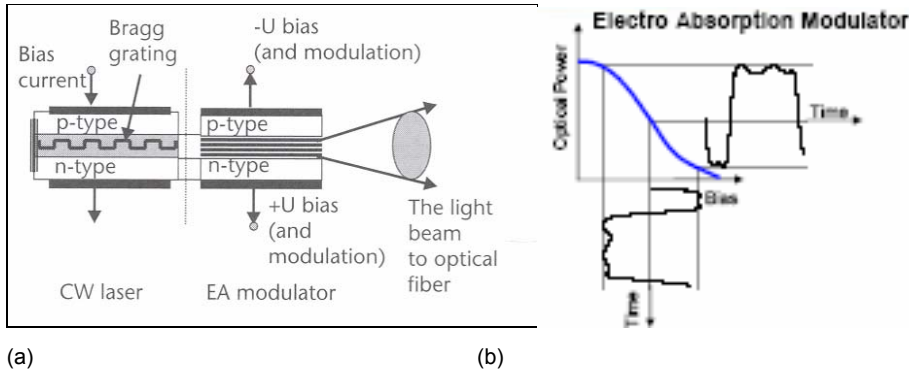
Figure 3- 1 (a) Structure of EA modulator (b) optical – electrical transfer characteristics (extracted from SHF AG information)

2.3.1   Mach Zehnder (MZ) Modulator

For 10 Gb/s or 40 Gb/s DWDM application, EO modulators are the technology of choice due to better performance in terms of chirp, extinction ratio (higher), and modulation speed compared to electro absorption devices. Over the years, lithium niobate ($LiNbO_3$) is the most popular material for electro optic modulators owing to its properties of enabling low loss waveguide and high electro optic effect. [6]. The most popular $LiNbO_3$ electro optic modulators nowadays employed particularly in high performance long haul optical transmission system are based on Mach Zehnder interferometric optical waveguide structure. The Mach Zehnder modulators has two pairs of electrodes deposited along the interferometer arms, one for DC bias voltage and the other for modulating signals. Meanwhile, numbers of DC bias voltage categorized the operation of Mach Zehnder modulators as single drive and dual drive.

Single drive MZIM

In a MZ modulator, the incoming light is split equally into two paths at Y branch (3 dB splitter) and traveled along upper and lower traveling wave electrode. An electric field is applied across the optical waveguide by electrode that generates change of refractive index of electro optic waveguide material via electro-optic effect. The change in the refractive index profile causes change of speed of light wave in the waveguide to change according to c/n_r [6], thus phase shift occurs. When the guided lightwaves from upper and lower waveguides recombine at the output Y branch, either a constructive or a destructive interference is generated depending on the relative phase shift of two branches. If the light waves from two arms are in phase, "ON" state of logic 1 is inferred due to constructive interference. The output is interpreted as "OFF" state or logic 0 if the light waves are π (or 180°) out of phase derived from destructive interference. If a coupler is placed at the Y-junction then naturally the constructive and destructive interference outputs can be obtained. These two outputs are then detected by a back-o-back connected photodetectors acting as a push-pull receiver.
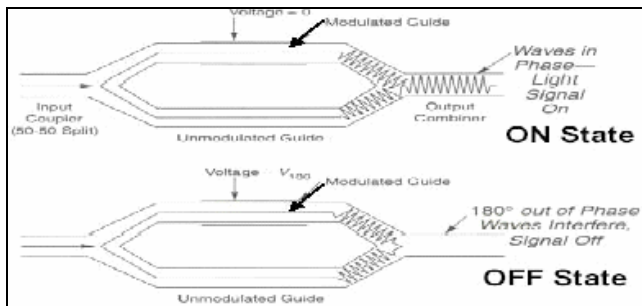
Figure 3- 2   Illustration of constructive and destructive interference at single drive MZ modulator output.(extracted from [7])

Combined optical wave at output of Y branch is described as [6]

_____   **9**

$$E_o = \frac{E_i}{2}\left[1 + e^{j\pi\frac{V(t)}{V_\pi}}\right] = E_i \cos\left(\frac{\pi}{2}\frac{V(t)}{V_\pi}\right)e^{j\pi\frac{V(t)}{V_\pi}} \tag{1}$$

To express in term of optical intensity to derive input-output transfer characteristic of MZIM[6]

$$E_o^2 = E_i^2 \cos^2\left(\frac{\pi}{2}\frac{V(t)}{V_\pi}\right) \tag{2}$$

Where E_o and E_i are the output and input electric field of the lightwaves, V(t) is the driving voltage or applied voltage at traveling eave electrode, Vπ is the voltage required to cause π phase shift of optical wave.
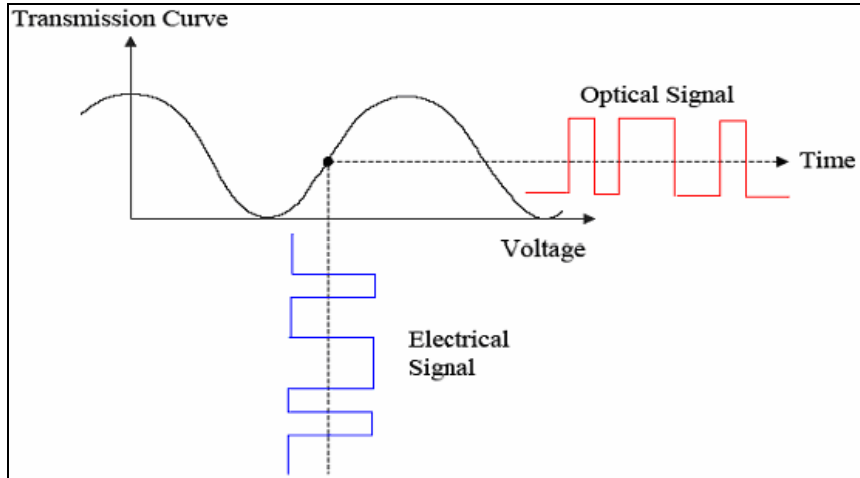
Figure 3- 3 The transmission curve of MZIM forms the periodic waveform as a function of applied biasing voltage.

As the transfer characteristic is $\cos^2$-shaped, the modulator will can biased in different region and modulating signal will be superimposed onto the bias voltage. The non linear transfer function has been used to generate non return to zero (NRZ), RZ pulse with various duty cycle, and DPSK signal.

Dual Drive MZIM
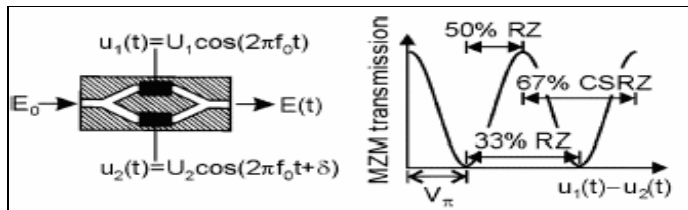
Figure 3- 4 Schematic and intensity transmission curve of a dual drive MZIM.

MZIM can also be driven with dual electrode structure or commonly referred as push pull modulator. In this report, we are considering chirp free driving by using two driving voltages with π phase difference [i.e $u_1(t)$ = -$u_2(t)$, δ= π]. The operational principle is similar to single drive MZIM but with both arms applied with voltage to phase modulate optical carrier via electro optic effect. Interference at output of Y branch will produce phase modulation. If the phase modulation is exactly equal in each path but opposite in sign, by combining two optical signals, the phase modulation is converted into intensity modulation. As a consequence, dual drive MZIM has an attractive feature; it can be driven as phase modulator and intensity modulator by changing its driving voltage. [8]

_____ **10**

4 TRANSMISSION LOSS AND DISPERSION

In an optical transmission system, optical fibers serve as medium to transport optical signals from source to destination. Due to low attenuation and ultra wide transmission bandwidth, optical fibers can transmit signals over long distances at high speed without amplification. Fiber losses impose a severe limitation on optical transmission because the signal power is greatly attenuated when reaching the receiver. With the advent of optical amplifiers, long haul transmission exceeding several thousands kilometers was achieved by compensating accumulated losses. However, the loss profile is imperative to determine spacing between amplifiers.[11] Fiber loss is expressed in units of dB/km by the following relationship

$$\alpha_{dB} = -\frac{10}{L} \log\left[\frac{P_T}{P_o}\right] \approx 4.343\alpha \qquad\qquad 3$$

where α = attenuation constant, P_T = transmitted power, Po = optical signal power at the input of a fiber of length L and Po is related to P_T by

$$P_T = P_o e^{-\alpha L}$$

4.1 Chromatic Dispersion

Chromatic dispersion severes the pulse distortion propagating through single mode fibers. The effect of chromatic dispersion can be expressed by expanding mode propagation constant β in a Taylor series about the center frequency ω_o [10]

$$\beta(\omega) = n(\omega)\frac{\omega}{c} = \beta_o + \beta_1(\omega - \omega_o) + \frac{1}{2}\beta_2(\omega - \omega_o)^2 + ... \qquad\qquad 4$$

$$\beta_m = \left[\frac{d^m\beta}{d\omega^m}\right]_{\omega=\omega_o} \quad (m = 0,1,2...)$$

Therefore we can obtain

$$\beta_1 = \frac{1}{c}\left(n + \omega\frac{dn}{d\omega}\right) = \frac{1}{\upsilon_g} = \frac{n_g}{c} \qquad\qquad 5$$

$$\beta_2 = \frac{d^2\beta}{d\omega^2} = -\frac{D\lambda^2}{2\pi c} \qquad\qquad 6$$

Where n = refractive index, c = speed of light, λ = operating wavelength, D = dispersion parameter expressed in units of ps/(nm.km). β_2 is an important factor known as the group velocity dispersion (GVD) because it accounts for the extent of optical pulse broadening on propagation inside the fiber.

The wavelength at where β_2 = 0 is called zero dispersion wavelength λ_D. Nevertheless, the dispersion is not eliminated completely at λ= λ_D because of higher order dispersive effects contributed by terms. Apparently, the main reason is the wavelength dependence of D. If we simulate the system in that particular region, the higher order effects should not be neglected and has to be taken into account by the dispersion slope expressed as [11]

$$S = \left(\frac{2\pi c}{\lambda^2}\right)^2 \beta_3 + \left(\frac{4\pi c}{\lambda^3}\right)\beta_2, \beta_3 = \frac{d^3\beta}{d\omega^3} \qquad\qquad 7$$

At $\lambda = \lambda_D$ where β2 = 0, S is proportional to β3. At $\lambda < \lambda_D$, the fiber exhibits normal dispersion. An interesting feature for the study of non linear effects should be noted at λ > λ_D where fiber displays anomalous dispersion. In fact, this region promotes propagation of solitons in optical fibers by supporting a balance between the dispersive and non linear effects.[10]

4.2 Non linear Effects

Nonlinear effects contribute to pulse distortion when optical power exceed several mW in a single channel optical transmission system due to their proportional relationship with the intensity of the EM field of propagating optical signal.[5] In spite of negative impacts such as signal crosstalk, optical signal power attenuation, and signal distortion, non linear effects can be exploited in curbing chromatic dispersion. Nonlinear effects can be categorized according to non linear refractive index or non linear optical signal scattering. The effects related to non linear refractive index compose of self phase modulation (SPM), cross phase modulation (XPM), and Four Wave Mixing (FWM). On the other hand, stimulated Raman Scattering (SRS) and Stimulated Brillouin Scattering (SBS) are affected belonged to non linear optical signal scattering caused by interaction between light and material.

In this report the SPM is the nonlinear effect of greatest concern because it is related to a single optical channel. SPM is a phenomenon caused by intensity dependence of the refractive index in non linear media that induce spectral broadening of optical pulses.[10]. When an optical pulse propagates along the fiber, refractive index of the fiber rises due to leading edge of the pulse. Conversely, falling edge of the pulse causes the refractive index of the fiber to decrease. As a result, a frequency chirp is introduced on both edge that interacts with the GVD to broaden the pulse. [12] . The SPM induced phase shift is expressed by [13]

$$\phi_{NL}(z,T) = |U(0,T)|^2 \frac{z_{eff}}{L_{NL}} \qquad\qquad 8$$

Where $z_{eff} = \frac{1}{\alpha}(1 - e^{-\alpha z})$, $L_{NL} = (\gamma P_o)^{-1}$, $\gamma = \frac{n_2 \omega_0}{c A_{eff}}$ and α = fibre attenuation constant, γ = non linearity coefficient, n_2 = non linear index coefficient

5   SIGNAL PROPAGATION MODEL

5.1 Nonlinear Schrodinger propagation equation

Signal propagation in optical fibers is the most important issue to be addressed in lightwave transmission systems. Optical pulses are subjected to linear and non linearities in the fibers. Linear degrading effects comprise of optical loss and GVD while non linearities include SPM, FWM, SRS and SBS effects. Interaction between these effects, including linear and non linear effects can cause temporal and spectral properties of the optical pulse to change significantly. A mathematical model commonly used to described the slowly-varying envelope of the optical field is Non linear Schrödinger equation (NLSE). The detailed derivations will not be discussed in this report but can be found in [10, 14, 15]. The general form of NLSE can be expressed by

$$\frac{\partial A}{\partial z} = -\frac{j}{2}\beta_2 \frac{\partial^2 A}{\partial T^2} + \frac{1}{6}\beta_3 \frac{\partial^2 A}{\partial T^3} + \frac{j}{24}\beta_4 \frac{\partial^4 A}{\partial T^4} - \frac{1}{2}\alpha A + j\gamma |A|^2 A - a_1 \frac{\partial}{\partial T}\left(|A|^2 A\right) - j\alpha_2 \frac{\partial}{\partial T}\left(|A|^2\right) \text{ (9)}$$

A = A (z, t) is slowly varying *complex* envelope of the optical signal, α = fiber loss, β2 and β3 are 2nd and 3rd order dispersion coefficient, γ = non linearity coefficient of fiber

When the pulses have duration over 1 ps, the NLSE can be simplified to

$$\frac{\partial A}{\partial z} = -\frac{j}{2}\beta_2 \frac{\partial^2 A}{\partial T^2} - \frac{1}{2}\alpha A + j\gamma |A|^2 A \qquad\qquad 10$$

For system to transmit at 10 Gb/s and above, the effects of third order dispersion has to be taken into consideration. By contrast, for system operating below 10 Gb/s, if the channel is not at λ_D, third order dispersion can be neglected.

5.2 Low Pass Equivalent Model

In developing low pass equivalent model of signal propagation in optical fibers, firstly, we have to assume that linear and non linear terms do not interact with each other. This is achieved by setting the power under certain threshold to prevent non linearity effect taking place. Hence, we can set γ = 0. Then, simplified model can be solved directly in the frequency domain to obtain

---

$$A(z,\omega) = \exp\left(-\frac{\alpha z}{2} - j\frac{\beta_2\omega^3 z}{2}\right)A(0,\omega) \qquad\qquad 11$$

Since A(z,ω) is fourier transform of A (z, t), the low pass equivalent model for single mode fiber transfer function is [16]

$$H(f) = \exp(-j\phi(f)) = \exp(-j\alpha f^2) = \exp\left(-j\left[\alpha B^2\left(\frac{f}{B}\right)\right]^2\right) \qquad\qquad 12$$

$\alpha = \pi D(\lambda)\dfrac{\lambda^2}{c}L$, $f = \upsilon - \upsilon_c$, B = data rate, f = frequency, α = attenuation constant, $D(\lambda)$ = chromatic dispersion, λ = operating wavelength, c = speed of light

Hence, the fiber is effectively a linear filter with attenuation and phase shift dependent on the transmission length.

5.3 Numerical SSF Method

When linear and non linear effects interact with each other, it is required to solve NLSE. However, NLSE is a non linear partial differential equation tha does not have analytical solutions except in some cases.[10, 14, 15] Hence, one of the method to solve the propagation problem is split-step Fourier (SSFT) method. SSFT method works on the following mechanism by firstly rewrite NLSE in the form[10]

$$\frac{\partial A(z,T)}{\partial z} = \left(\hat{D} + \hat{N}\right)A \qquad\qquad 13$$

$\hat{D}$ and $\hat{N}$ are dispersion operator and non linear operator which are given by

$$\hat{D} = -\frac{j}{2}\beta_2\frac{\partial^2}{\partial T^2} + \frac{1}{6}\beta_3\frac{\partial^2}{\partial T^3} - \frac{1}{2}\alpha \text{ and } \hat{N} = j\gamma\left[|A|^2 + \frac{\partial i}{\omega_o A}\frac{\partial}{\partial T}\left(|A|^2 A\right) - j\alpha_2\frac{\partial}{\partial T}\left(|A|^2\right)\right]$$

Assume the dispersive and non linear effects act independently, the fiber length is divided into many sections spaced h apart. Each section is split into two segments with h/2 respectively. The optical pulse is propagated for a segment using Fast Fourier Transform (FFT) algorithm and equation below.

$$\exp\left(h\hat{D}\right)A(z,T) = F^{-1}\exp\left(h\hat{D}j\omega\right)F[A(z,T)] \qquad\qquad 14$$

where $\hat{D}(j\omega) = \dfrac{j\beta_3}{2}\omega^2 - \dfrac{\alpha}{2}$ is dispersion operator in Fourier domain and F and F⁻¹ indicate Fourier and inverse Fourier transformations.

At z+h/2, optical field is multiplied by non linear term where the non linearity is assumed to take place at the mid place of each section. Eventually, optical is propagated thorugh h/2 again to complete a whole section to obtain the following equation.

$$A(z + h_n, T) = \exp\left(h\hat{N}\right)F^{-1}\exp\left(h_n D(\hat{j}\omega)\right)F[A(z,T)] \qquad\qquad 15$$

SSFT is widely used in pulse propagation solution due to its fast execution. The relative faster speed by up to two orders of magnitude is attributed to the used of FFT algorithm that speed up numerical evaluation.[10] Accuracy of this method is justified by the selection of step sizes and T. Depending on the application of individual problem, reducing step sizes is necessary to improve the accuracy of numerical simulations. As suggested by Agrawal, window size of typically 10-20 times the pulse width should be wide enough to ensure pulse energy confined within the window. Otherwise, numerical instabilities may occur.

_____ **13**

6   MODULATION FORMATS

Optimal modulation formats play essential role to combat linear and non linear impairments, particularly in ultra long haul lightwave transmission systems. An optimal modulation format is responsible to carry the maximum bit rate with narrow optical spectrum to enable closer channel spacing in DWDM system. Furthermore, high tolerance to chromatic dispersion effect and robustness to nonlinearities such as SPM, XPM and FWM are major properties to pursue. The format should also be compatible with the detection scheme in order to minimize receiver renovation and thus increase cost effectiveness.

In this report, the modulation formats covered were Non return to zero (NRZ or NRZ-ASK), Return to zero (RZ or RZ-ASK), NRZ- DPSK, RZ-DPSK (including carrier suppressed RZ-DPSK) and duobinary. Although NRZ and RZ are not advanced modulation formats, they have been used explicitly in conjunction with DPSK formats to develop a generic photonic transmitter based on the fundamental optical principles. In this section, the basic generation principles and characteristics of these five modulation format will be discussed and their applications in developing simulator will be described in next section.

6.1   NRZ or NRZ-ASK

For simplicity, we would refer NRZ-ASK to NRZ since they are fundamentally similar. NRZ has been the dominant modulation format in the last two decades due to its simplicity to generate, detect and have compact spectra. On top of that, it can attain high sensitivity with Erbium doped fiber amplifiers (EDFAs). Although higher bit rates demand is taxing the limit of NRZ signaling where new schemes are being deployed to replace NRZ, it served as a good reference for the purpose of comparison.

NRZ data is encoded by the following logic. A "zero" is a low logic level and "one" is a high logic. Figure below shows the NRZ signal corresponds to the logic level.
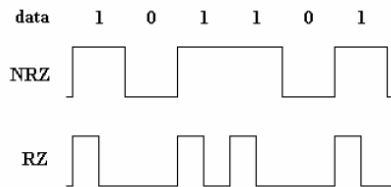
Figure 6- 1 NRZ and RZ line coding for 101101 data sequence.
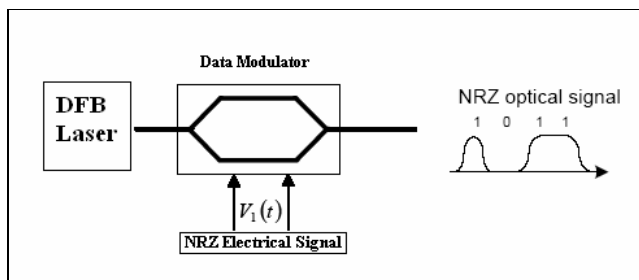
Figure 6- 2 Block diagram of NRZ photonic transmitter.

A CW laser is injected from DFB laser source into MZ modulator. The modulator is biased at linear region and driven with $V\pi$. The modulator acts as an intensity modulator to convert NRZ electrical signal with data rate B into ASK optical signal at the same rate. Due to non linear characteristics of the modulator, the NRZ optical signal usually have better Q factor than the electrical signal. The optical spectrum of B data rate NRZ signal will have signal bandwidth of B Hz.
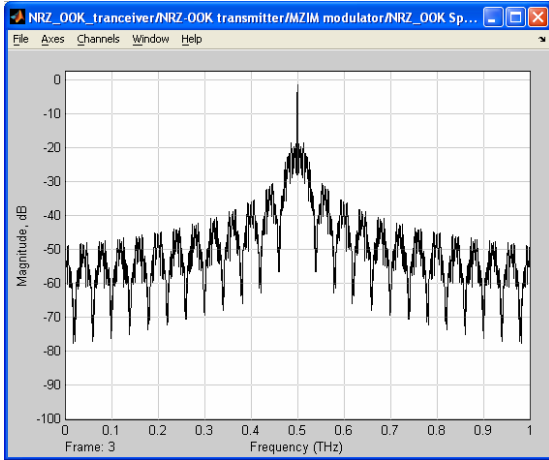
Figure 6- 3 Optical spectrum of NRZ at carrier of 500 GHz.

6.2   RZ (or RZ-ASK)

RZ-ASK, also known as Return to zero (RZ) pulses has several advantages over NRZ signals. The advantages are attributed to how RZ handle the optical power. As illustrated in Figure 6- 1 , the power level of RZ pulses always return to zero even when successive logic 1 bits occur.
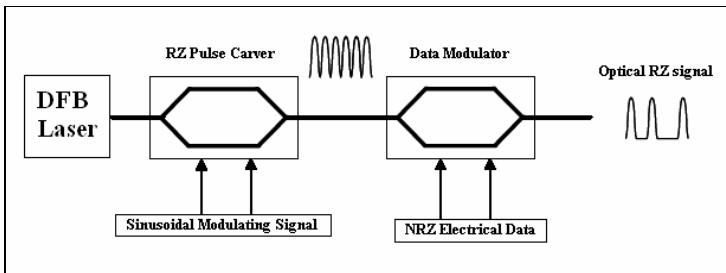
Figure 6- 4 Block diagram of RZ photonics transmitter.

Firstly, to generate opticl RZ pulses, a MZ modulator commonly known as pulse carver is fed with sinusoidal electrical signal to "carve" pulses from optical CW carrier wave. The optical RZ pulse train is then fed into another MZ modulator known as intensity modulator to modulate the electrical data on the RZ pulses. There are a number of variations in RZ format based on the biasing point in transmission curve shown in Table 1.

Biasing point in Transmission Curve	RZ generation Characteristics
	Biasing point: Maximum, V2π Drive signal amplitude: 2 Vπ Drive signal frequency: 20 GHz Pulse width: 9 -10 ps RZ pulse frequency: 40 GHz frequency doubling effect.

LN Binh, H.S. Tiong and T.L. Huynh "40Gb/s amplitude and phase modulation optical fibre transmission systems: PART I : SIMULINK Modeling, ©**Monash University 2005**

	Biasing point: Linear region, Vπ/2
	Drive signal amplitude: Vπ
	Drive signal frequency: 20 GHz
	Pulse width: 9 -10 ps
	RZ pulse frequency: 20 GHz
	Biasing point: Minimum, Vπ
	Drive signal amplitude: 2 Vπ
	Drive signal frequency: 20 GHz
	Pulse width: 9 -10 ps
	RZ pulse frequency: 40 GHz frequency doubling effect. (Carrier suppressed RZ is generated using this scheme)

Table 6-1 Summary of RZ format generation and characteristics of single drive MZIM based on biasing point, drive signal amplitude and frequency.[17]

RZ has a wider spectrum than NRZ due to its narrower pulse width but CSRZ has eliminated this inherent disadvantage. CSRZ has optical phase difference of π in adjacent bits, remove the optical carrier component in optical spectrum and reduce the spectral width.
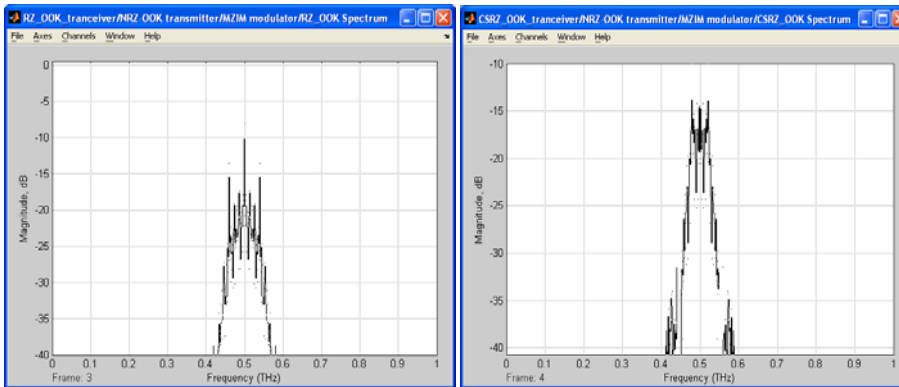
(a)   (b)

Figure 6- 5 Optical spectra of (a) RZ and (b) CSRZ at carrier of 500 GHz.

6.3   Differential Phase Shift Keying (DPSK)

Information encoded in the phase of an optical carrier is commonly referred to as optical phase shift keying. In early days, PSK requires precise alignment of the transmitter and demodulator center frequencies. [18] Hence, PSK system is not widely deployed. With DPSK scheme introduced, coherent detection is not critical since DPSK detection only requires source coherence over one bit period by comparison of tow consecutive pulses.

A binary 1 is encoded if the present input bit and the past encoded bit are of opposite logic and a binary 0 is encoded if the logic is similar. This operation is equivalent to XOR logic operation. Hence, an XOR gate is usually employed in differential encoder. NOR can also be used to replace XOR operation in differential encoding.

In optical application, electrical data "1" is represented by a π phase change between the consecutive data bits in the optical carrier, while state "0" is encoded with no phase change between the consecutive data bits. Hence, this encoding scheme gives rise to two points located exactly at π phase difference with respect to each other in signal constellation diagram.
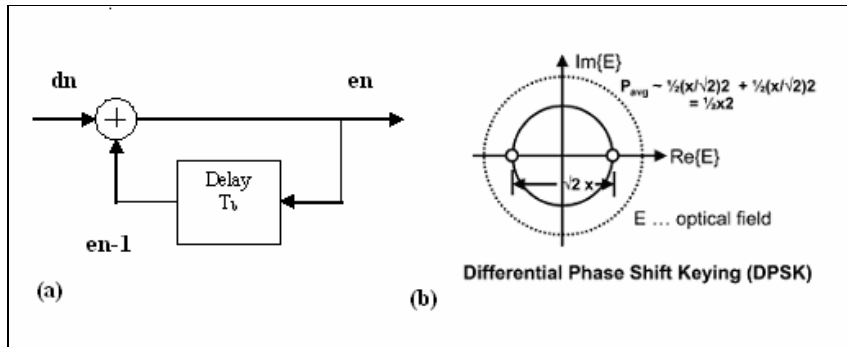
Figure 6- 6 (a) The encoded differential data are generated by $e_n = d_n \oplus e_{n-1}$ (b) Signal constellation diagram of DPSK.[1]

3.6.1   NRZ-DPSK
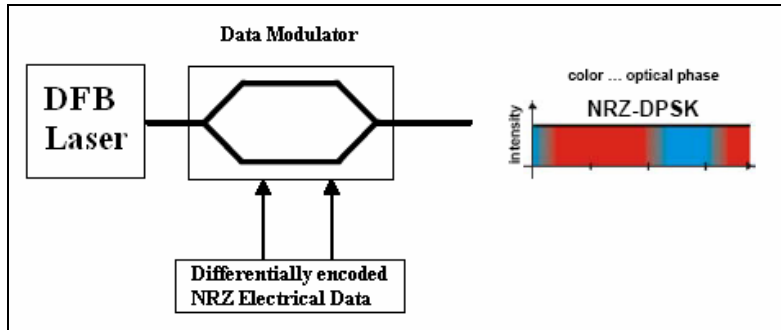
Figure 6- 7 Block Diagram of NRZ-DPSK photonic transmitter.

Figure above shows the block diagram of a typical NRZ-DPSK transmitter. Differential precoder of electrical data is implemented using the logic explained in Section 6.3. In phase modulating of optical carrier, MZ modulator known as Data Phase Modulator is biased at minimum point and driven by data swing of 2 Vπ. The modulator showed an excellent behavior that the phase of the optical carrier will be altered by π exactly when the signal transiting the minimum point of the transfer characteristic.

3.6.2 RZ-DPSK
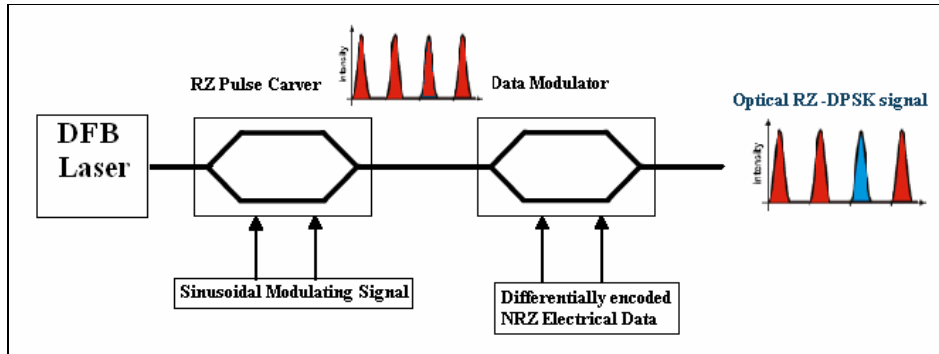
Figure 6- 8 Block diagram of RZ-DPSK photonics transmitter.

Setup of RZ-DPSK transmitter is essentially similar to RZ-ASK with Data intensity modulator replaced with Data Phase Modulator. The difference between them is the biasing point and the electrical voltage swing. Different RZ formats can also be generated according to Table 6-1.

7   RECEIVER

The receiver structure is dependent on modulation format imposed on optical carrier. If ASK and duobinary formats are used, single photodiode direct detection receiver is usually employed to convert the optical signal power into electrical signal by photodiode. The single photodiode direct detection scheme is depicted in diagram below.
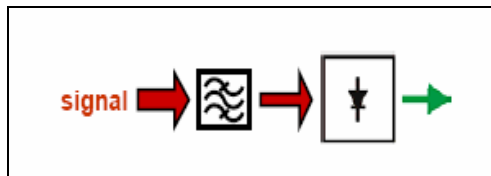
Figure 7- 1 Single photodiode direct detection receiver. [1]

DPSK receiver requires an optical preprocessing stage to accomplish demodulation. The optical signal is first passed through a MZ delay interferometer (MZDI) which has a differential delay equal to a bit period. The delay is achieved by extending the second path of MZ arm approximately λ_{bit} as shown in Figure 7- 2 . Since in practice, exact delay is too difficult to construct, a heating element is applied on the interferometer arm to fine ture the differential phase delay.
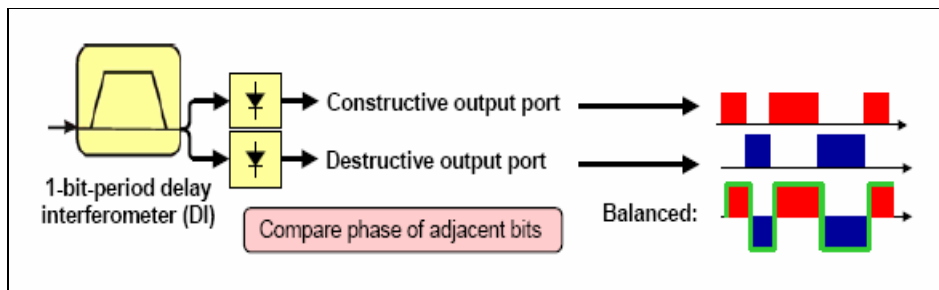
Figure 7- 2 Balanced detection with delay demodulation using two photodiode direct detection. [1]

When there is no phase change between adjacent bits, maximum power appears at the constructive port. When the phase in adjacent bit differs by π, maximum power exists at the destructive port. Hence, the

preceding bit served as a phase reference for demodulating the current bit.[1] As a result, the bit coherency is only required for two bit periods.

Under DPSK modulation and demodulation scheme, both constructive port and destructive port carry similar but logically inverted data stream. Therefore, they can be either detected by themselves ("single-ended detection") or balanced. Single ended detection simply uses a photodiode to convert the optical signal power at either port to electrical signal. Balanced detection is completed by connecting two photodiodes and processed digitally.

8   SIMULINK MODELS

Analytical engineering approach to identify optimization parameter especially in long haul communications system may impose limitations on number of optical channels as well as distances. Since the interaction of these parameters may give hundreds of even thousands of combinations, computer-aided engineering approach provide assistance in terms of accuracy and speed from precise engineering point of view. There are a number of computer based programs and simulation tools available to achieve optical system design modeling. These packages offer various benefits depending on the applications and situations investigated. Some of them provide click-and-drop interface and some of them are closed to user's intervention.

Matlab Simulink is one of the most user-friendly software platforms that can write the simulation software using different building blocks and tools. Simulink provide a set of libraries that contain digital signal processing block set, mathematical fundamentals and electronic modules. Hence, it is open for optical module modeling which is crucial in our applications to model the components from physical level to system level. The flexibility of the simulation by appropriate sampling techniques enhances the integration of optical module modeled at physical operating principle such as optical modulator with mathematical model that is required to solve fiber propagation equations.
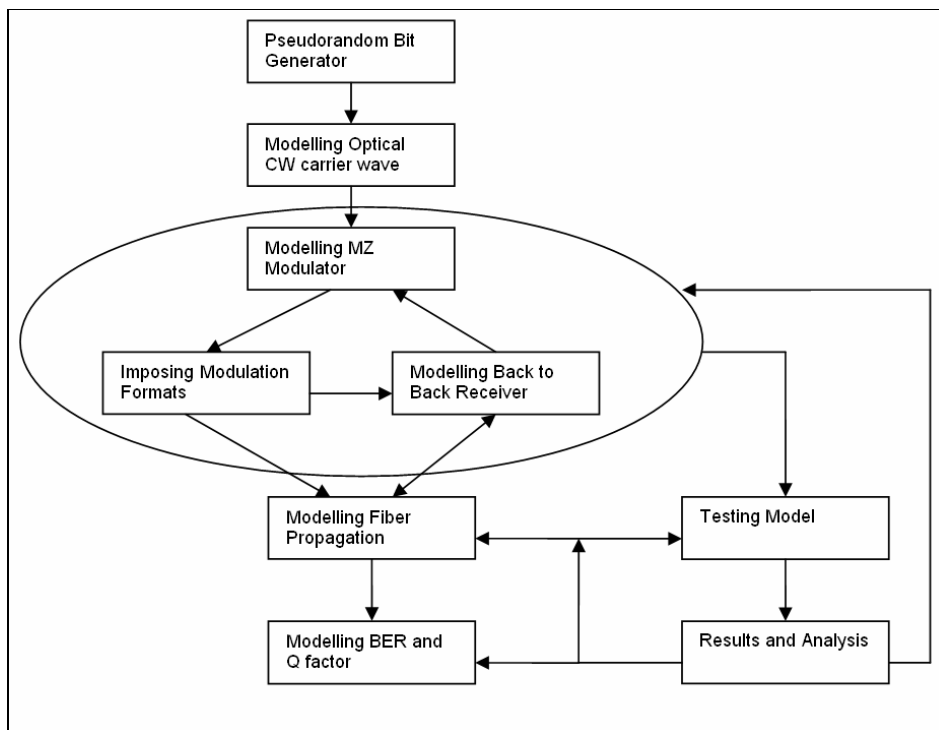
Figure 8- 1 Flow Diagram of simulator design processes.

The design processes depicted in Figure 8- 1 illustrated how 40 Gb/s photonic transmitter were designed and tested. Firstly, pseudorandom bit generator can be easily modeled using Bernoulli Binary Generator provided

LN Binh, H.S. Tiong and T.L. Huynh "40Gb/s amplitude and phase modulation optical fibre transmission systems: PART I : SIMULINK Modeling, ©**Monash University 2005**

in communication blockset. Optical CW carrier wave which was assumed to be DFB laser as explained in 3.1 was modeled readily by sine wave in signal processing blockset. Three circled processes exposed a circular procedure that required constant testing and feedback from results and analysis. Often, the design on MZ modulator had to be adapted, modified, and implemented both with mathematical model and physical operating principles. The modulator model would have to be confirmed with the modulation format as well as receiver to demodulate the signal. When modulation formats were compatible with back-to-back receiver, propagation model was developed to test the system performance with BER model. This process would consume a lot of time as system grew in complexity, a slight change in model would alter the result significantly. During the design process, results were collected to gain information and feedback on necessary model alteration and confirmation. The rest of this section will discuss modeling process and present the results from time to time to demonstrate the working principles of the model. Although the developed model can generate different modulation formats, only RZ-DPSK results including eye diagrams, time scope and spectrum scope for demonstration purpose.

8.1   Bernoulli Binary Generator
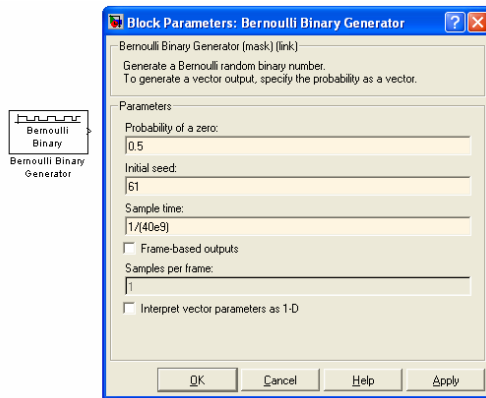
Figure 8- 2 Block parameters setup and block diagram of Bernoulli Binary Generator in Simulink. Probability of a zero is set to 0.5 and sample time is set to 25 ps to output 40 Gb/s data sequence.
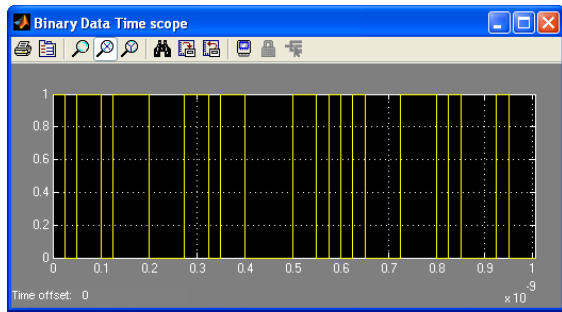
Figure 8- 3 Binary datas in 1 ns generated by Bernoulli Binary Generator.

8.2 DFB laser
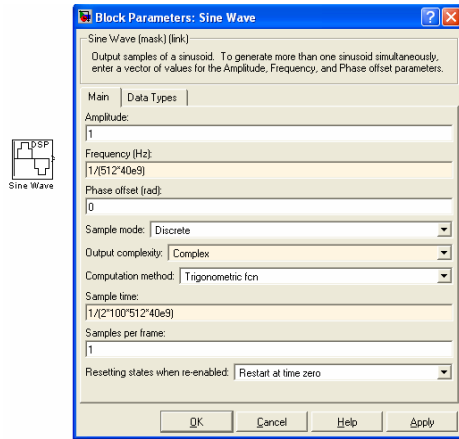
Figure 8- 4 Block parameters setup and block diagram of DFB laser in Simulink.

Optical carrier frequency set in this case is 2.048 THz. It is different from 193 THz (1550 nm) because 2^n x Data rate of optical carrier will simplify calculation in setting up eye diagram parameters since we can compute exactly number of cycles of sinusoidal sine wave in a bit period. Sample mode was set to discrete due to similar reason stated previously. Sample time was relatively subject to how accurate we require the optical carrier to be, typically 200 samples in a frame is substantial to produce a clean and nice wave.
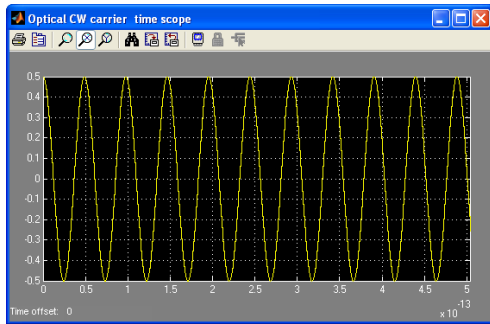
Figure 8- 5 Optical CW carrier wave at 2.048 THz shown in 0.5 ps time span.

8.3 Mach Zehnder Interferometric Modulator

MZ interferometric modulator model was developed based on the principle explained in 0. Implementation can be divided into intensity modulator and phase modulator depending on the biasing voltage and voltage swing. Hence, the model was developed based on the pulse carver applications.

3.8.1 Pulse Carver

Since optical phase distortions (such as chirp) will affect DPSK receiver performance, dual drive MZIM pulse carver was required to operate in perfect push-pull operation. In other words, sinusoidal electrical signals amplitude has to be similar and of exact opposite phase. This requirement is difficult to achieve in practice but fairly straightforward in simulation environment. Assume extinction ratio is large, optical field exiting a dual drive MZIM is described mathematically[1]

$$E(t) = \frac{E_o}{2}\left\{\exp\left[j\pi\frac{u_1(t)}{V_\pi}\right] + \exp\left[j\pi\frac{u_2(t)}{V_\pi}\right]\right\} \approx E_o \exp\left[j\pi\frac{u_1(t)+u_2(t)}{2V_\pi}\right] \times \cos\left[\pi\frac{u_1(t)-u_2(t)}{2V_\pi}+\varphi\right]$$

16

Where E0 is magnitude of input optical field, Vπ is the electrical voltage to produce π phase shift in either of modulator's two arms, φ is the relative optical phase between 2 arms without electrical drive signals; u1(t) = $U_1\cos(2\pi f_m t)$; u2(t)= $U_1\cos(2\pi f_m t + \theta)$ and fm is the electrical signal frequency.

Since chirp free driving condition required u1(t)=-u2(t), Equation (3) can be reduced to

$$E(t) \approx E_o \cos\left[\pi \frac{u_1(t) - u_2(t)}{2V_\pi} + \varphi\right]$$

17

Let $\varphi = \frac{\varphi_1 - \varphi_2}{2}$ where $\varphi_1 = \pi \frac{V_{DC1}}{V_\pi}$ and $\varphi_2 = \pi \frac{V_{DC2}}{V_\pi}$. By incorporating optical carrier frequency into (16), optical field exiting dual drive MZIM can be re-expressed as [19]

$$E(t) = E_o \left\{\cos\left[2\pi f_c t + \alpha\pi \cos(2\pi f_m t) + \varphi_1\right] + \cos\left[2\pi f_c t + \alpha\pi \cos(2\pi f_m t + \theta) + \varphi_2\right]\right\} \text{ (18)}$$

Where fc is the optical carrier frequency, α = $\pi \frac{U_{1,2}}{V_\pi}$ (assigned as the modulation index) The mathematical analysis shows that the biasing voltage, Vπ is reduced by half with respect to single drive MZIM, thus with driving voltage as well, an advantage using balanced modulator structure.
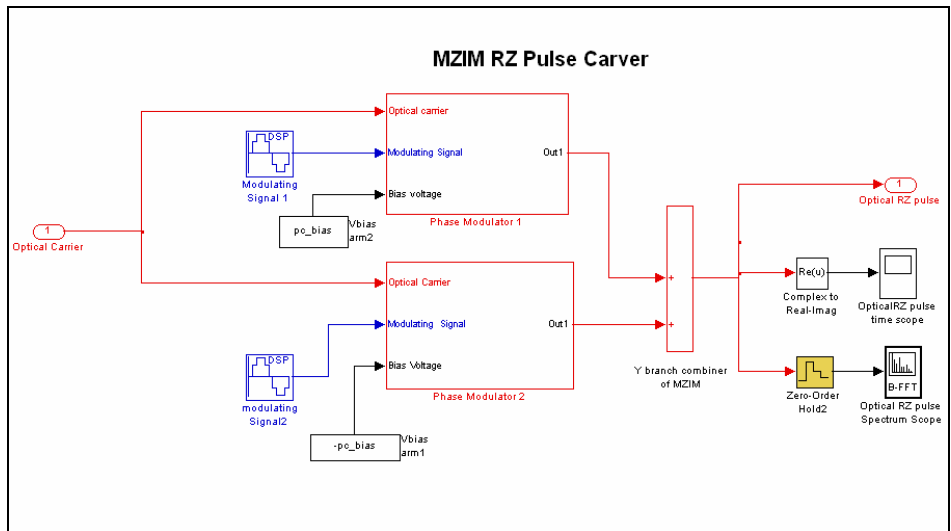
Figure 8- 6 Dual drive MZIM pulse carver.

The MZIM had two arms biased at voltage set by pc_bias, and modulated by two modulating signal with exact π difference between them to create push-pull configuration. The output of each arm was combined using sum that act like a coupler so that they can interfere constructively and destructively. The output was monitored using a time scope and spectrum scope.

(a)   (b)
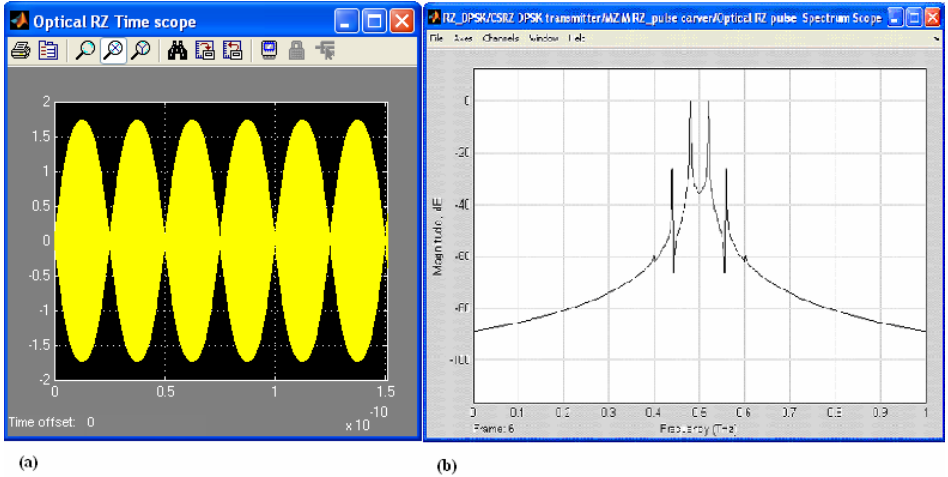
Figure 8- 7 (a) carrier suppressed RZ pulse in time domain. The pulse is 25 ps wide with carrier reside in the pulse at 2.048 THz. (b) Spectral characateristics of CSRZ pulse. The carrier was shown clearly being eliminated at 500 GHz.
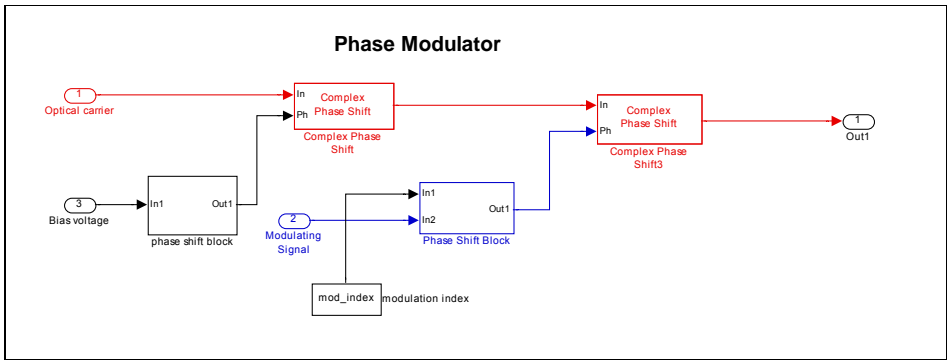
Figure 8- 8 One of the phase modulator arms in Figure 8- 6 .

Figure 8- 8 showed the equally split optical carrier signal enter one of MZIM path. Biasing voltage was fed to create a relative phase reference for electrical modulating signal. Electrical signal was used to modulate optical carrier signal with phase relative to biasing voltage phase. This model essentially represented one of the two cosine terms in (18. Hence, if MZ interferometric structure was discarded, this model alone acted like a phase modulator.
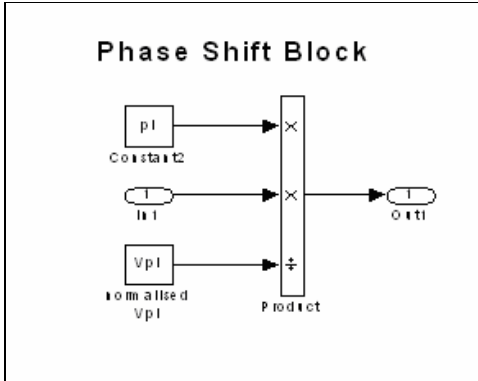
Figure 8- 9 One of the phase shift block in **Figure 8- 8** . A direct mathematical model derived for phase implementation..

Biasing Point	Parameters Setting	
	Arm 1	Arm 2
Linear	Modulation index: pi/4 Signal frequency: 40 GHz Biasing voltage: Vπ/4 Phase Offset: pi/2	Modulation index: pi/4 Signal frequency: 40 GHz Biasing voltage: -Vπ/4 Phase Offset: pi+pi/2
Minimum (CSRZ)	Modulation index: pi/3 Signal frequency: 20 GHz Biasing voltage: Vπ/2 Phase Offset: 0	Modulation index: pi/3 Signal frequency: 20 GHz Biasing voltage:-Vπ/2 Phase Offset: pi
Maximum	Modulation index: pi/2 Signal frequency: 20 GHz Biasing voltage: Vπ Phase Offset: pi/2	Modulation index: pi/2 Signal frequency: 20 GHz Biasing voltage: -Vπ Phase Offset: pi/2

Table 8-1 Parameters setting for three formats of RZ pulses.

3.8.2 Data Modulator
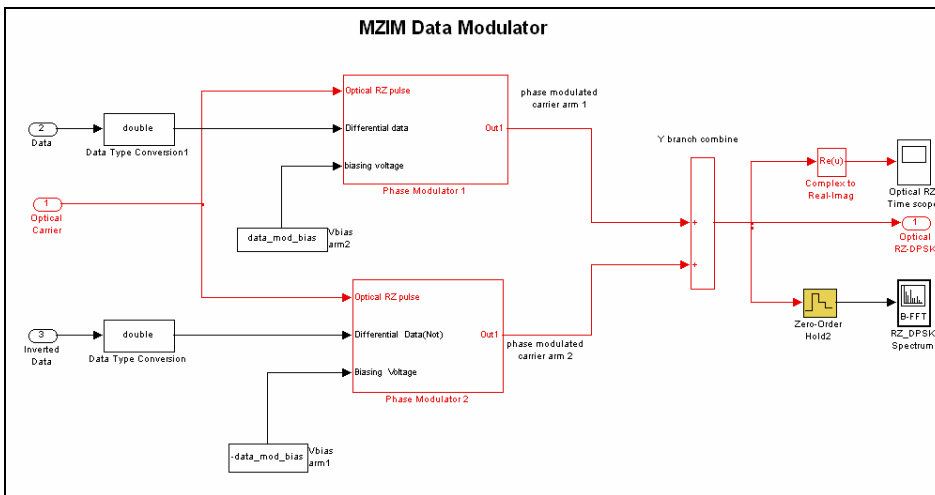
Figure 8-10 Data modulator based on dual drive Mach Zehnder interferometeric structure driven by data and inverted data.

Data modulator based on MZIM structure employed similar model as in pulse carver. However, when the MZIM model was driven as PSK data modulator, the biasing voltage was always Vπ/2 and Vπ/2 data voltage swing. Phase modulation would be limited to 0 and π, equivalent to signal constellation diagram in Figure 6-6 and double in frequency of driving data. If other than PSK modulation format was imposed, the biasing voltage and data voltage swing will be different and based on what were explained in 6.

Before feeding into phase modulators, there was a data type conversion to convert data in Boolean form generated by Bernoulli generator to double type to be processed by phase modulator model. Phase modulator was similar to that of Figure 8-8. Logically, they were similar but phase shift block was slightly altered to assemble data modulation principle in this model.
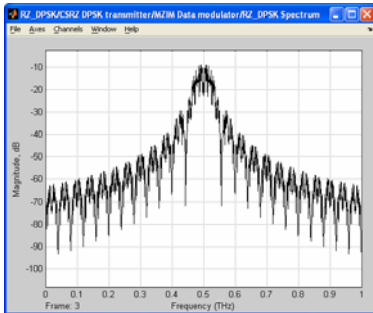
Figure 8-11 Spectrum scope of monitored after data modulator using CSRZ-DPSK modulation format with carrier of 500 GHz.
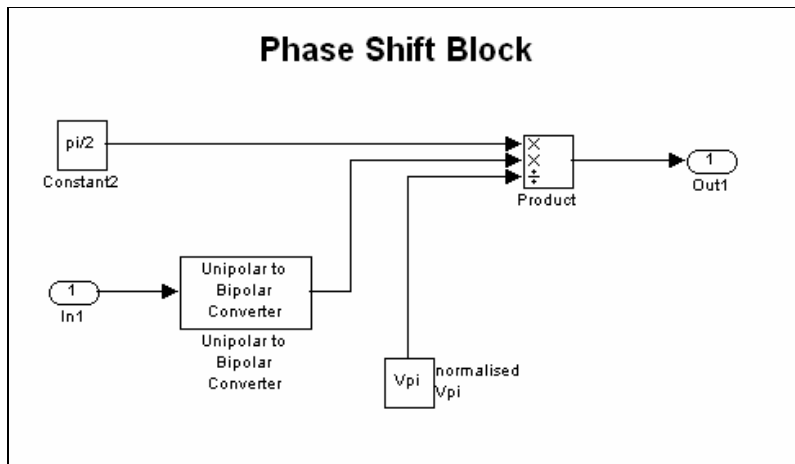
Figure 8-12 Second phase shift block in one of the phase modulator arm in **Figure 8-10**.

8.4   Differential Data Encoder
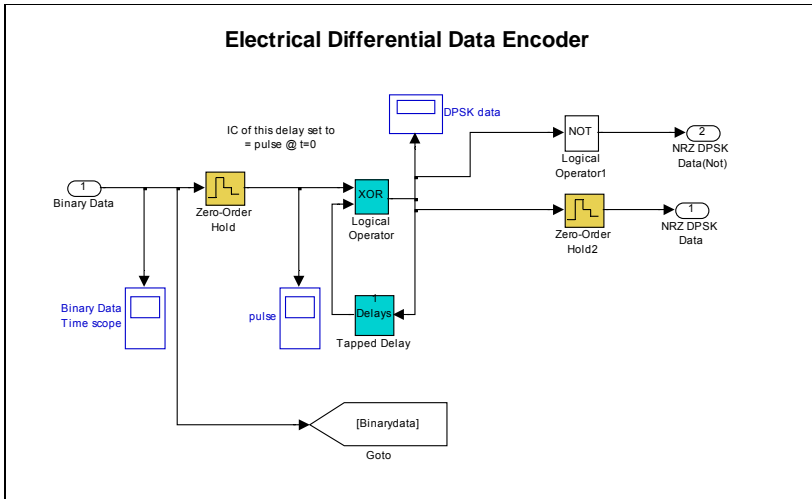
Figure 8- 1 3 Electrical differential data encoder.

Differential data encoder was implemented using differential encoding logic described in 6.3. Bernoulli binary generator was driven at 20 Gb/s and sampled at the same frame rate to XOR with the past encoded bit. This model consists of two NRZ DPSK data output complement with each other which are necessary to operate dual drive MZIM modulator.
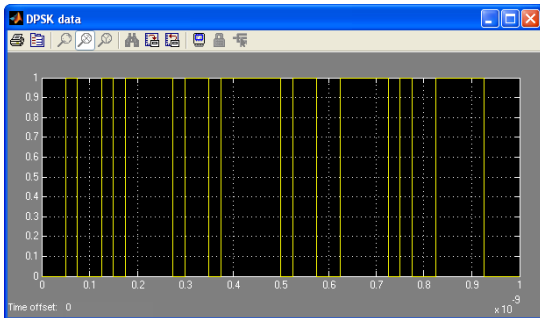
Figure 8- 1 4 Differential encoded binary data in Figure 8- 3 .
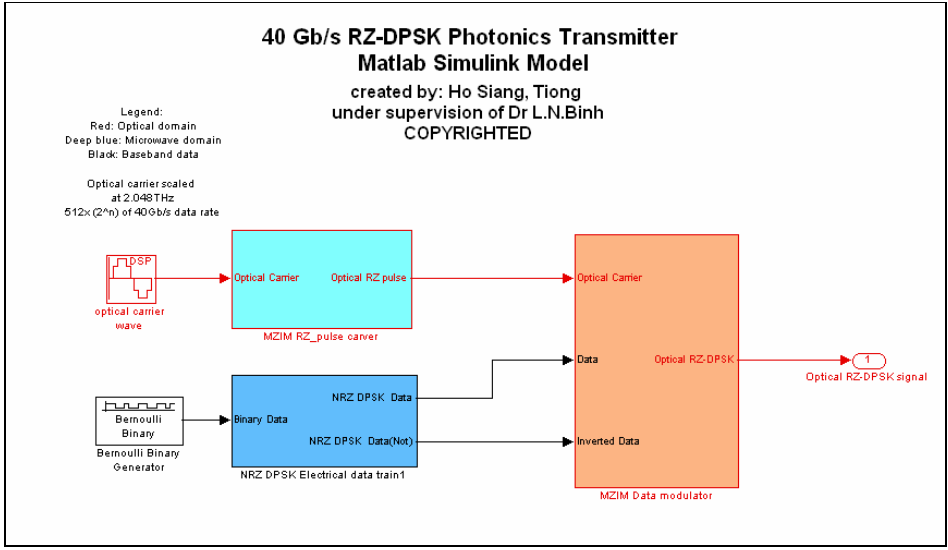
Figure 8-１５A complete Simulink model of photonics transmitter.

8.5 Back to back receiver
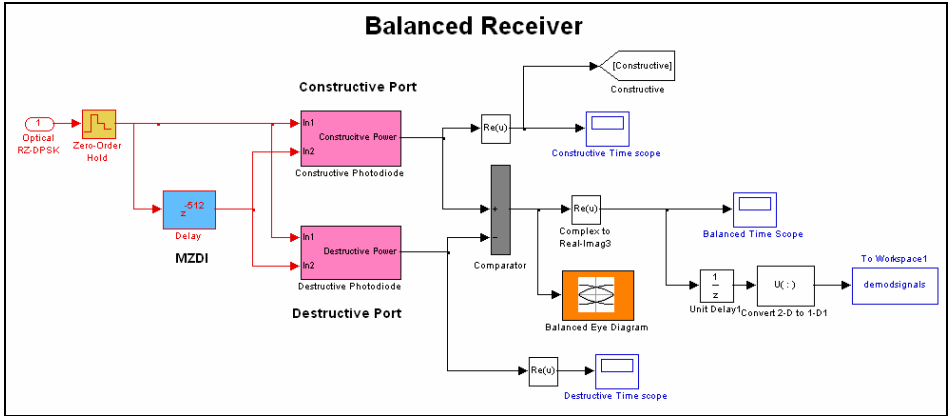
Figure 8-１６Simulink model of balanced receiver.

Balanced receiver was constituted by a MZDI model, 2 photodiode models, and a comparator with time scopes and eye diagrams to evaluate performance. MZDI was implemented by delay block provided in Simulink library. Since optical carrier wave was calculated in discrete size of 2^n x 40e9, it was simple to calculate exactly number of samples required to delay in a bit period. For instance in this case, 2^n = 512, therefore, delay samples were 512 in order to delay a bit period.

_____ **27**
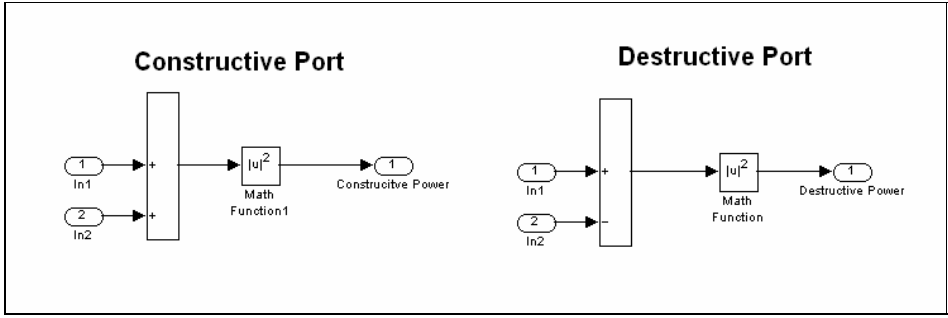
Figure 8- 1 7 Constructive and destructive port in balanced receiver. Math function magnitude^2 represents the photodiode.

Constructive and destructive interference of received signal and a-bit-delay signal were implemented by addition and subtraction respectively. When there is no phase change between adjacent bits, addition will constructively superpose two signals. Conversely, subtraction will superpose two signals with π phase shift. Since photodiode converted optical power to electrical signal, it could be modelled as magnitude^2 function.

Single ended detection would require either of one of the port to be detected using eye diagram block. On the other hand, balanced detection would require subtraction (logically) between two outputs before detected by eye diagram.
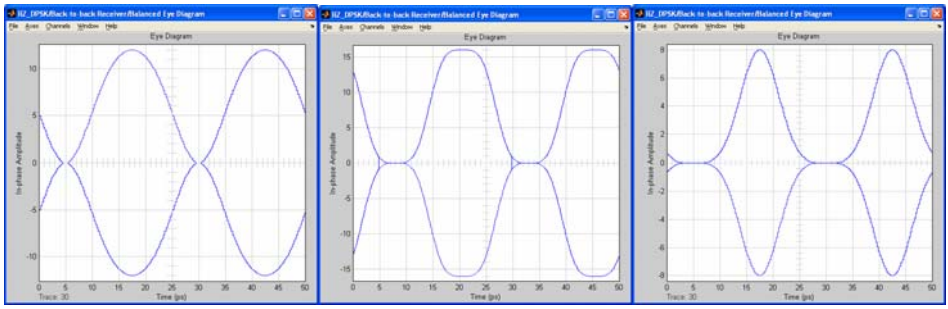
Figure 8- 1 8 Eye diagrams of 3 different RZ modulation formats detected by back to back balanced receiver. From left to right, CSRZ, 50 % RZ, 33% RZ.

5.8.1   Eye Diagram
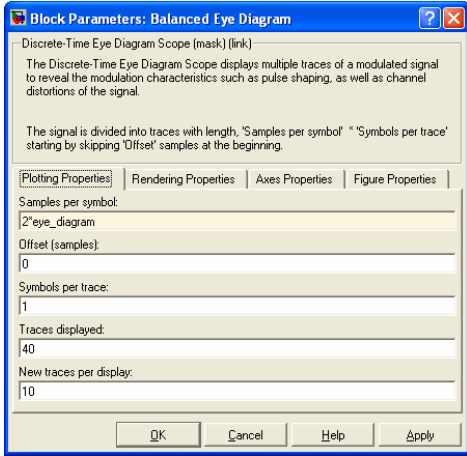
Figure 8-19 Parameter settings for eye diagram

Samples per symbol was set by carrier frequency x bit period. As shown in Figure 8-19, 2*eye_diagram implied eye diagram display two bits period. Hence, it can be adjusted accordingly to view over number of bit period.

8.6   Signal Propagation
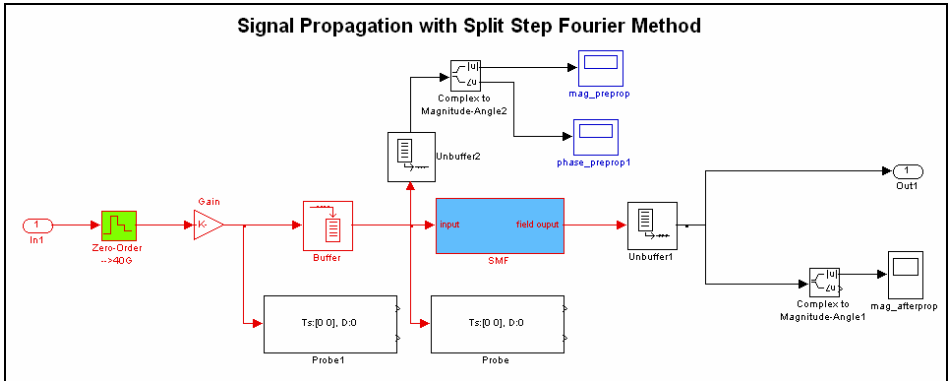
Figure 8-20 Simulink model of signal propagation in fiber.

The zero order hold (sampler in green colour) is used to obtain pulse envelope of the optically modulated signal. The signal propagation model could only deal with pulse envelope since it was developed using split step Fourier method to solve NLSE equation which the signal was assumed to have slow-varying time envelope as explained in 5.3. Gain acted like an attenuator to control the power input to the fiber. Buffer was not in actual practice but it was necessary to specify number of bit samples in a particular FFT window. The buffered signal was input to SMF block to be processed by a MATLAB function ssprop_matlabfunction_modified.m.
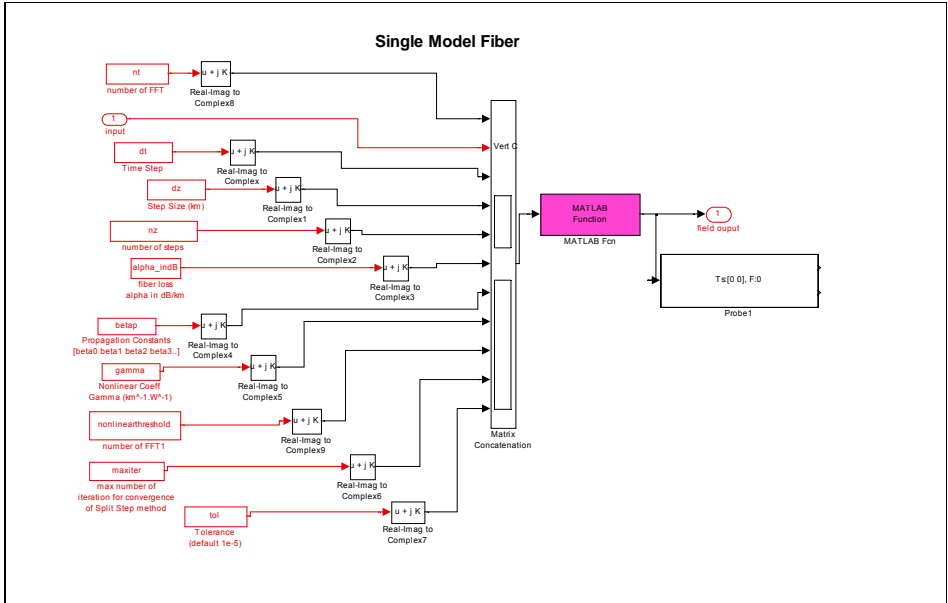
Figure 8- 2 1 Parameters setting in SMF block.

In SMF block, the signal was concatenated by the parameters such as, number of FFT, time step, step size, number of steps, fiber loss constant, propagation constants, non linear coefficients. The signal was processed by MATLAB function ssprop_matlabfunction_modified.m which implemented the split step Fourier algorithm.
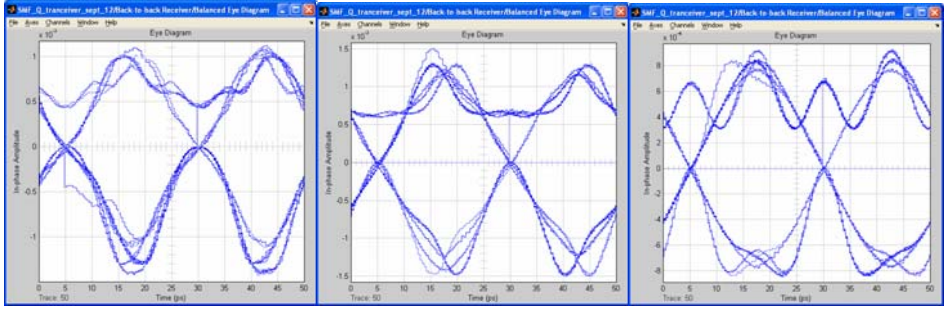
Figure 8- 2 2 Eye diagrams of 3 different RZ modulation formats after 2 km fiber propagation using balanced receiver. From left to right, CSRZ, 50 % RZ, 33% RZ.

8.7   Bit error rate (BER)

Bit error rate was calculated by using MATLAB programs developed by Dr Binh and Liem. The histogram was first computed using histogram.m and a sample result of histogram after 2 km fiber span was illustrated in diagram below. Q factor and BER were calculated using BER_GaussianQ.m by assuming the signal distortion due to fiber propagation was Gaussian distributed.
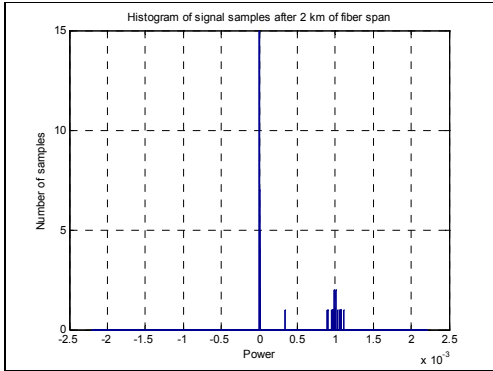
Figure 8- 2 3 Histogram of signal samples after 2 km of fiber span detected at constructive port using CSRZ-DPSK modulation format.

9   RESULTS AND COMPARATIVE STUDY OF DIFFERENT MODULATION FORMATS.

9.1   Novelty of Developed Photonics Transmitter

The novelty of the developed photonics transmitter, especially Mach Zehnder interferometric modulator (MZIM) is the ability to generate different modulation formats based on physical structure and biasing voltage of the transmission system.

1.9.1   NRZ or NRZ ASK

(a)   (b)

LN Binh, H.S. Tiong and T.L. Huynh "40Gb/s amplitude and phase modulation optical fibre transmission systems: PART I : SIMULINK Modeling, ©**Monash University 2005**
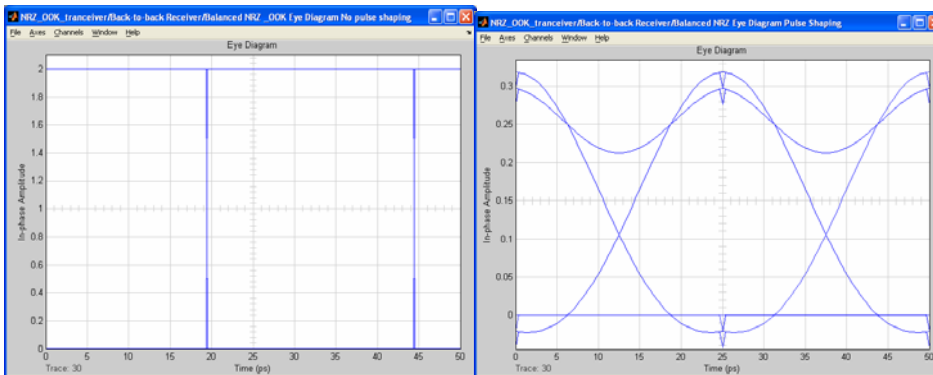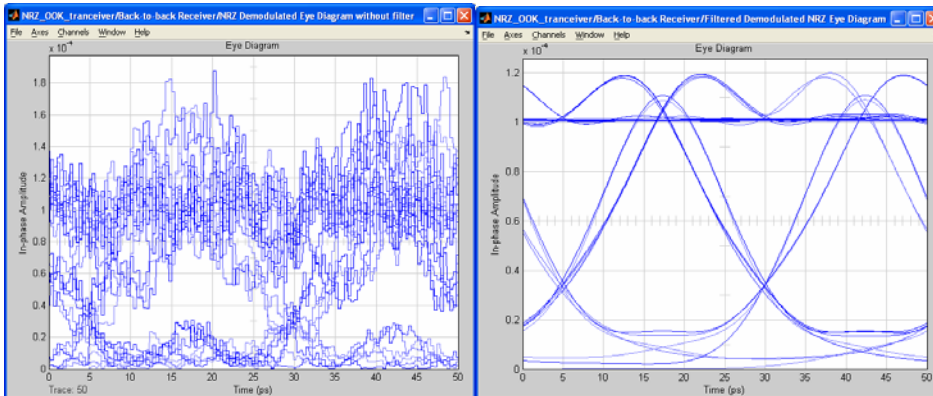
(c)   (d)

Figure 9- 1 NRZ eye diagrams (a) back to back without filtering (b) back to back with Gaussian filtering (c) after 3 km SMF without filtering (d) after 3 km SMF with Gaussian filtering

1.9.2   RZ or RZ-ASK
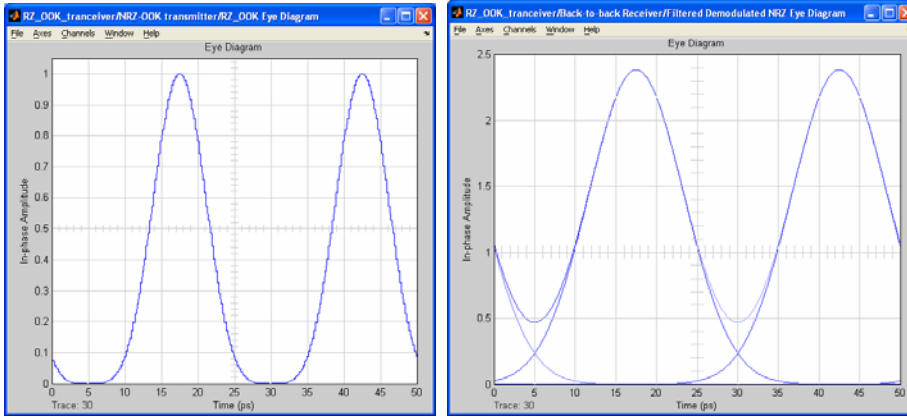
(a)   (b)
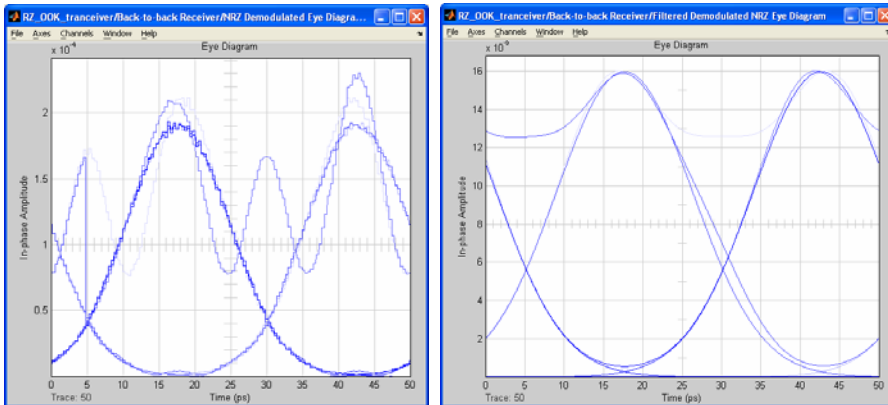
(c)   (d)

Figure 9- 2 33 % RZ eye diagrams (a) back to back without filtering (b) back to back with Gaussian filtering (c) after 2 km SMF without filtering (d) after 2 km SMF with Gaussian filter.

1.9.3   NRZ-DPSK

(a)

(b)

(c)

(d)
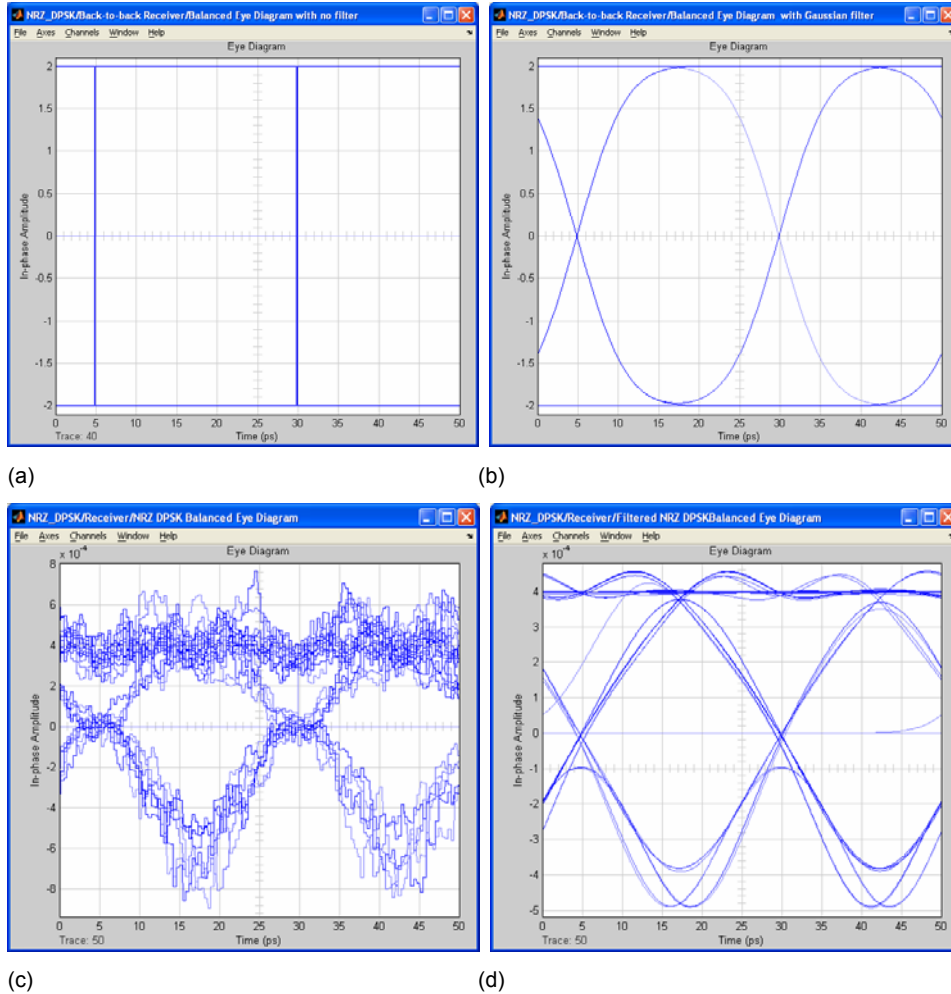
Figure 9- 3 NRZ-DPSK eye diagrams (a) back to back without filtering (b) back to back with Gaussian filtering (c) after 3 km SMF without filtering (d) after 3 km SMF with Gaussian filtering

1.9.4   RZ-DPSK
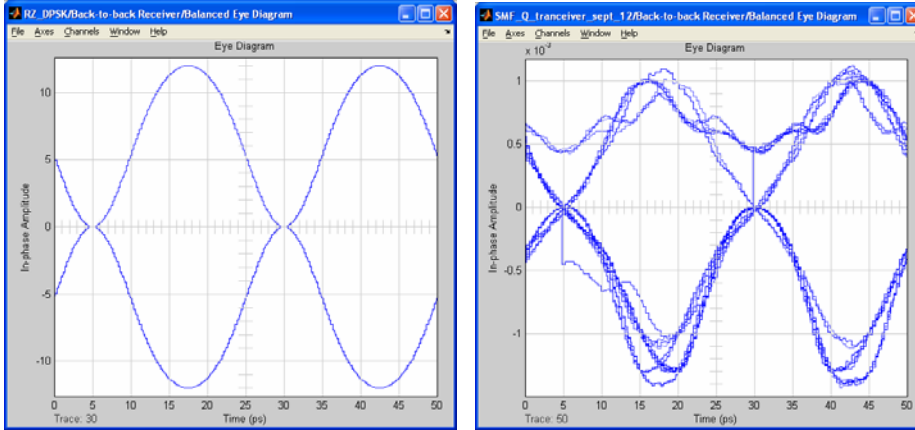
(a)   (b)

Figure 9- 4 RZ-DPSK eye diagrams (a) back to back without filtering (b) back to back after 2 km SMF

1.9.5   Spectra of Modulation Formats

The optical carrier frequency has been scaled down to 500 GHz instead of 193.1 THz (1550 nm). Spectrum range of scope reveals only a whole spectral width from DC (frequency = 0) to sampling frequency specified in front of the scope. Hence, optical carrier frequency at hundreds of THz required a sampling frequency just as high but at the expense of spectral resolution. For illustration purpose, using carrier frequency of 500 GHz portrays the optimum spectral property of each modulation formats. The feasibility of this method was confirmed by testing the spectrum at different frequencies (500 GHz ±100 GHz) and all the results were identical. PRBS length is 2^7-1.
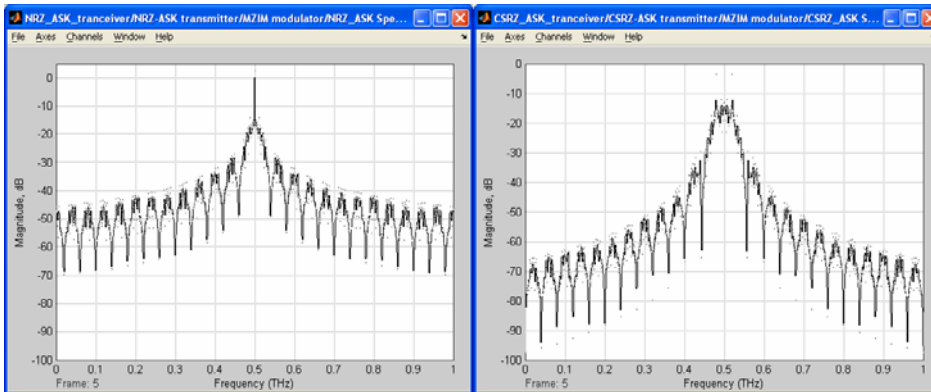
(a)   (b)
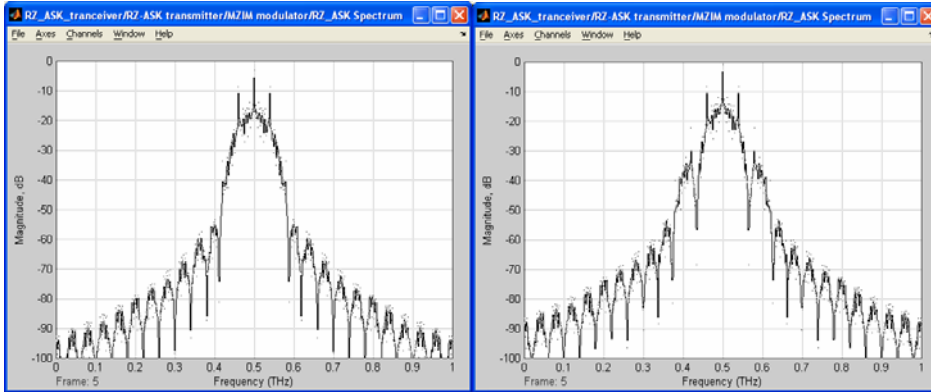
(c)   (d)

Figure 9- 5 Optical spectra of transmitted signal of (a) NRZ-ASK (b) carrier suppressed RZ-ASK (c) 33 % RZ-ASK (d) 50%RZ-ASK
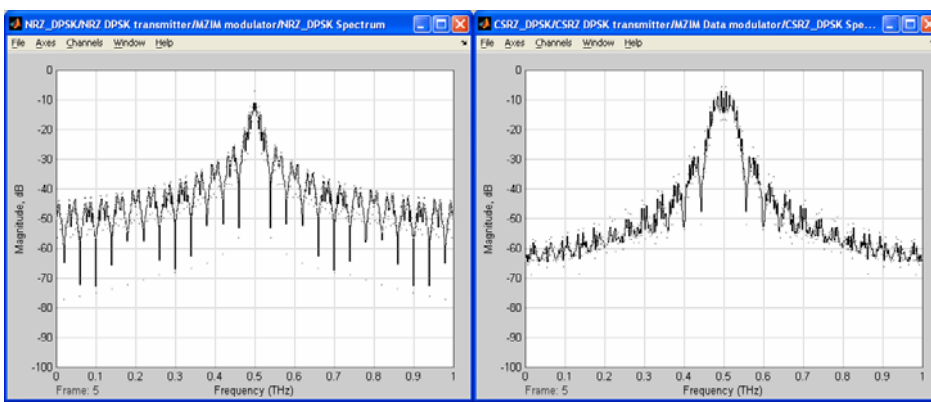
(a)   (b)
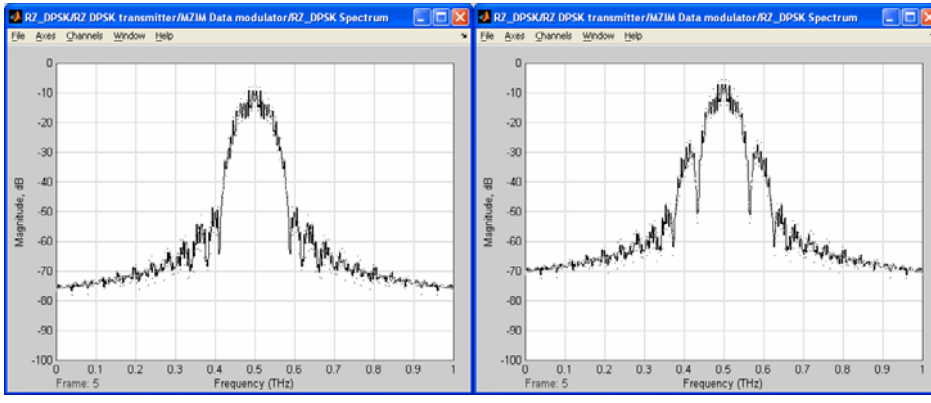
(c)   (d)

Figure 9- 6 Optical spectra of transmitted signal of (a) NRZ-DPSK (b) carrier suppressed RZ-DPSK (c) 33% RZ-DPSK (d) 50%RZ-DPSK .

From the Fourier transform, the bit duration is inversely proportional to signal bandwidth in frequency.[21] It is clear to show that RZ in both ASK and DPSK format have wider main lobe than NRZ. 33% RZ pulse has the widest main lobe of about 80 GHz (considered single side band) due to the shortest bit duration whereas carrier suppressed RZ has the narrowest signal bandwidth.

ASK modulation showed impulse at the carrier frequency in NRZ and RZ line coding. Impulse of carrier frequency in NRZ-ASK is the highest among three formats of RZ-ASK because the intensity of RZ always return to zero, thus the power resides in carrier frequency will be less than that of NRZ. As implied by its name, CS-RZ has no impulse at its carrier frequency due to alternate inversion of polarity at adjacent bits which removes the carrier in the spectrum "virtually". On the other hand, there is no impulse found in DPSK modulation format using either NRZ or RZ line coding. It is contributed by the DPSK format itself because the data sequence is encoded in alternate polarity as shown in Figure 6- 6 . Hence, the carrier impulse power could be shifted and distributed to the main lobe and side lobe as we could observe that the signal power spectra of NRZ and RZ-DPSK formats having approximately 5 dB above that of the ASK.

When considering the harmonics or side lobes, the NRZ-ASK and DPSK have higher number and power of side lobes. For RZ, side lobes in DPSK have lower number and significant reduced power compared with ASK. Carrier suppressed RZ in DPSK and ASK has a larger percentage of total power contained in the side lobes compared with 33% and 50% RZ which was also reported in [22].

From the analysis above, we can conclude that although RZ occupies a wider signal bandwidth than NRZ, carrier suppressed RZ has a more compact spectrum comparable to NRZ. In addition, CSRZ has removed carrier impulse in spectrum. However, CSRZ has larger percentage power contained in side lobes compared with other forms of RZ. Fortunately, with optimal bandpass filtering, the concern is addressable.

9.2   System performances

The simulation was conducted with FFT window length of 2048 samples with each bit period correspond to 64 samples that was equivalent to 32 bits. The transmitter and balanced receiver were assumed to be perfectly tuned so that any mismatch between two signal paths could be neglected. The received signals were not filtered. Amplified spontaneous emission (ASE) noise was not included since no amplifier was considered in the system. Although it is known that probability density function of DPSK is not Gaussian,[20] for simplicity, we would assume the model of Q has Gaussian distribution. No forward error correction (FEC) and PRBS length of 2^7-1 was employed.
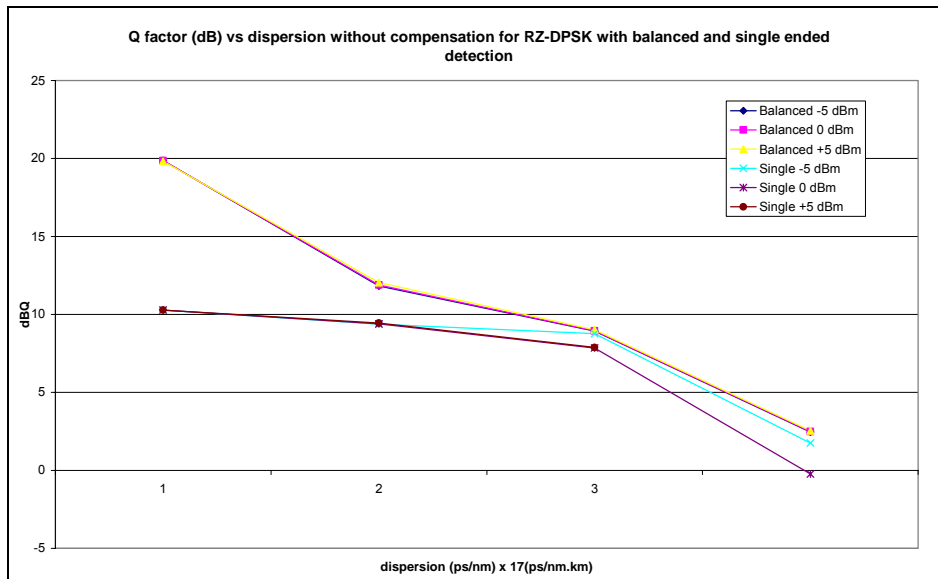
Figure 9- 7 Balanced and single ended detection performance for single channel 33 % RZ-DPSK system with various fiber input power.

Figure 9- 7 showed that balanced detection outperformed single ended detection in DPSK modulation scheme. The advantage has been confirmed by several papers.[1, 11, 18, 21]Balanced receiver utilizes signal power from two paths effectively but single port receiver rejects half of the signal power. The power loss is equivalent to 3-dB power penalty.[11] On the other hand, increasing fiber input power for balanced detection has no obvious impact on chromatic dispersion and SPM penalty whereas penalty increased after 2 km fiber span for single ended detection. It should be noted here that when other non linearities like XPM and FWM were considered, further penalty could be imposed on single ended detection. Hence, it can be deduced that balanced detection is important to utilize DPSK effectively in suppressing chromatic dispersion and non linearities in fiber.

10 log (Q) vs dispersion without compensation
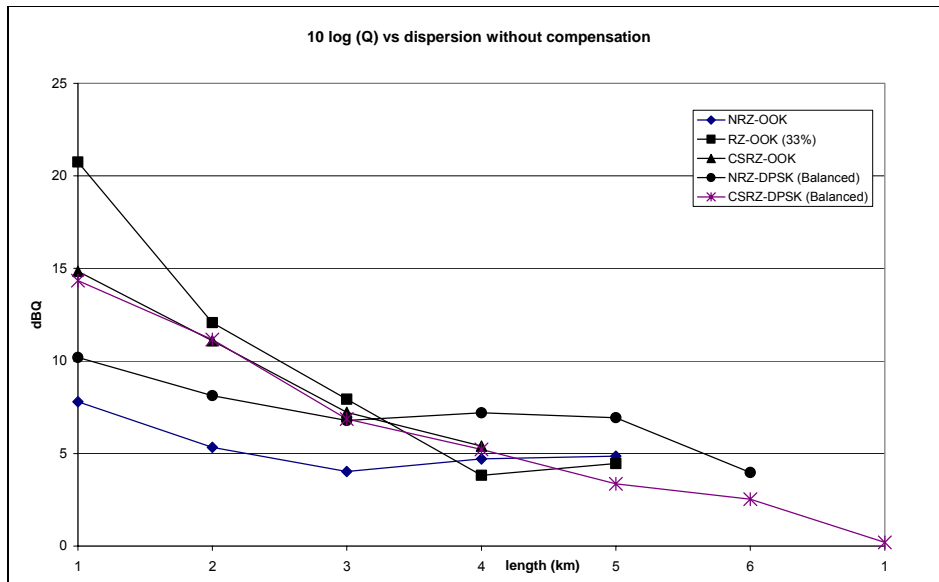
Figure 9- 8 Chromatic dispersion induced single channel performance for NRZ-ASK, NRZ-DPSK, RZ-ASK, RZ-DPSK, CSRZ-ASK and CSZR-DPSK. Fiber input power was set at -10 dBm.

To compare NRZ-ASK and NRZ-DPSK, it was clear that DPSK with balanced detection has 3-dB better of dispersion tolerance performance as explained before. On the other hand, if we compare CSRZ-DPSK and CSRZ-ASK, 3-dB advantage was not present. As reported in [20], DPSK system will not outperform ASK system without non linear phase noise. The key advantage of RZ only becomes significant when self-phase modulation and amplified spontaneous emission (ASE) were taken into consideration. In this case, since only chromatic dispersion was considered, 3-dB advantage was only apparent in NRZ-ASK and NRZ-DPSK system.
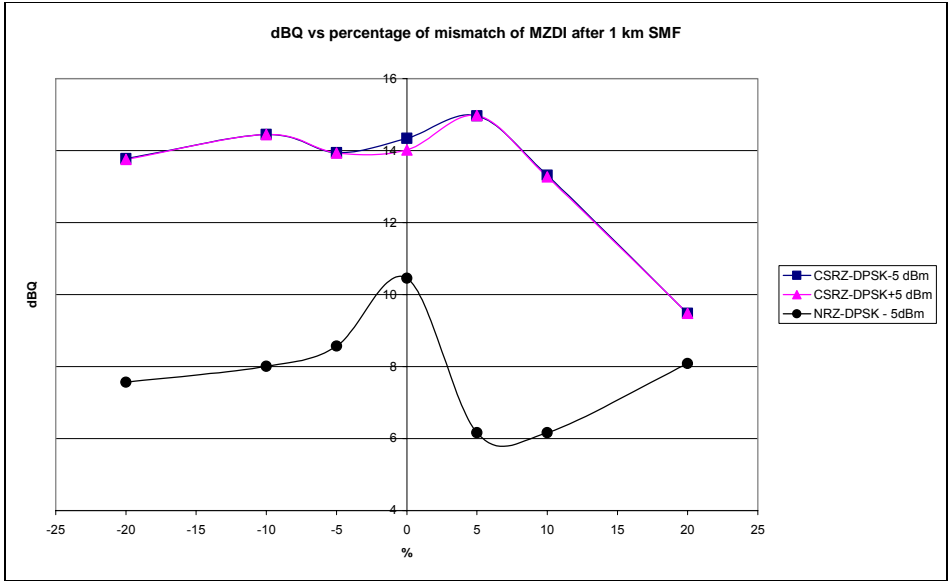
Figure 9- 9 Performance of CSRZ-DPSK and NRZ-DPSK in dispersion tolerance against percentage of mismatch in MZDI after 1 km of SMF.
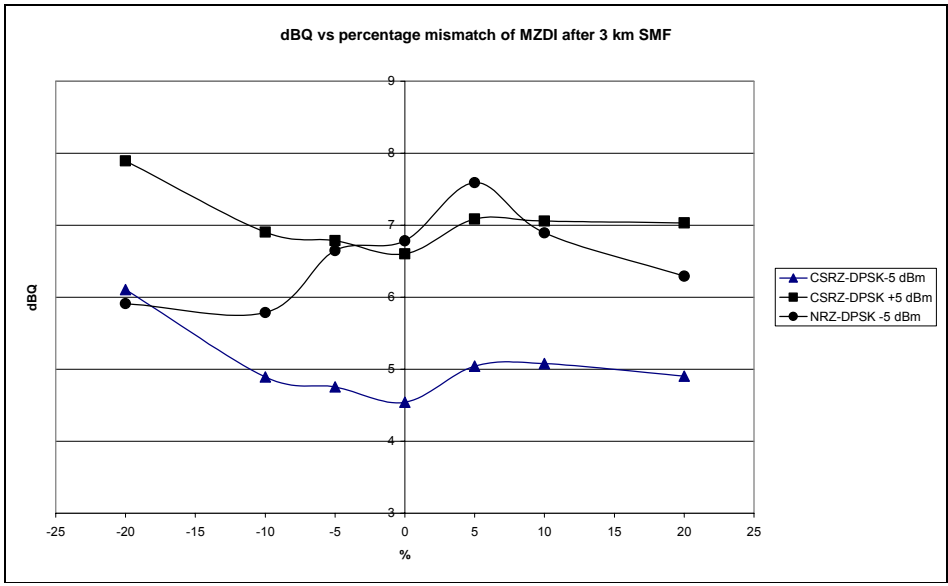
Figure 9- 1 0 Performance of CSRZ-DPSK and NRZ-DPSK in dispersion tolerance against percentage of mismatch in MZDI after 3 km of SMF.

From Figure 9- 9 and Figure 9- 1 0 , it can be shown that there is no apparent penalty within ±5% of mismatch between two paths in MZDI. At +5%, there were 5 results displaying higher Q value which might imply a slight mismatch in MZDI could be beneficial. Nevertheless, the result could be optimistic due to finite samples in a bit period in this simulation, 512 samples in a bit. A more accurate result could be obtained by applying higher samples in a bit (2^n, n = 1,2,3…) despite the need to compromise the speed of simulation. Beyond the range of ±5%, inconsistent dBQ showed that higher mismatch percentage will eventually cause critical issue in

demodulating received signals. In fact, there are a lot of factors affect the accuracy of the result, especially Q factor evaluation which will be discussed in the following section.

9.3   Discussions

The system performances depicted in 9.1 had a few discrepancies with the simulated results of other papers. [1, 3, 7, 19, 20] The discrepancies could be largely due to some limitations of the model and speed of simulation.

The largest discrepancy is the performance of RZ-DPSK over RZ-ASK. RZ-DPSK was reported to have outperformed RZ-ASK,[18] especially in non linear regime of long haul transmission systems. Therefore, computation of BER based on Gaussian noise distribution was invalid.[22] It was reported by Bosco et al that the non linear systems could model optical noise as Gaussian distributed to obtain fairly accurate result but only consider parametric amplification.

Apart from that, 3-dB advantage of DPSK over ASK is derived from a larger separation between the two transmitted symbols in DPSK (2sqrt(E_b)) and ASK (sqrt($2E_b$)) when the same average signal power is used. Nevertheless, we found that this explanation did not apply both to NRZ DPSK and RZ DPSK system. As reported in [18], 3 –dB advantage was obtained if the channel is assumed to be linearly dominated by ASE noise. Then, optical noise could be modeled as classical additive Gaussian noise. However, if non linearity tolerance was taken into credit, since SPM caused by Gordon-Mollenauer effect is very intensity dependent, conventional Q-factor failed to predict the SPM penalty because conventional Q-factor underestimates the system performance in linear regime and overestimates non linear regime.[18] As a result, it was proposed by C. Xu et al[18] that a differential phase Q-factor was more appropriate to estimate performance of balanced detected DPSK signals.
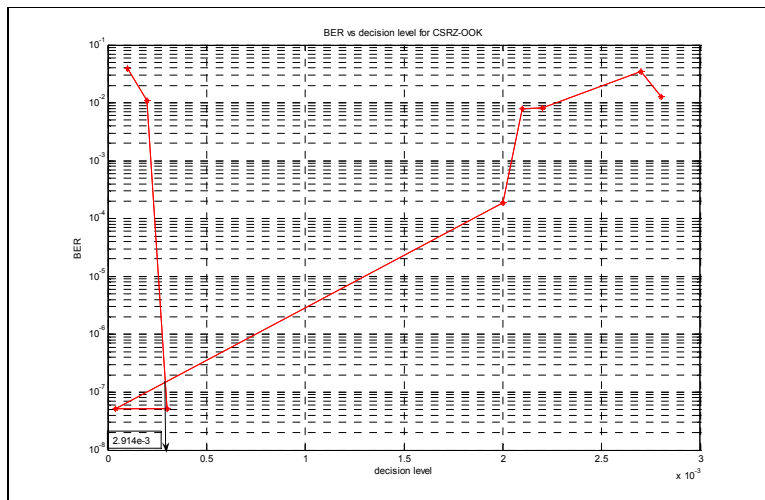
Figure 9- 1 1 Determination of optimum threshold level for CSRZ-ASK.

Optimum decision threshold played a vital role in obtaining an accurate Q factor, especially for ASK system. At optimum threshold, based on the Gaussian intensity distribution of the received signal, Q factor can characterize the statistical fluctuation of the received signal fairly well but not with DPSK system. It is one of the reason proposed to have contribute to the insignificant advantage of RZ-DPSK over RZ-ASK in Figure 9- 8 . For explanation purpose, only CSRZ-ASK was depicted in Figure 9- 1 1 to determine optimum threshold level. The BER against different decision levels were plotted to give a V shape graph. The intersection was identified as the optimum threshold in determining Q factor.

10   CONCLUDING REMARKS

Based on the Simulink platform, an optical transceiver simulator for different modulation format in single channel transmission link has been successfully developed. The simulator focused on three major components, photonic transmitter, optical fiber and optical receiver particularly Mach Zehnder delay interferomeric balanced receiver.

The novelties of this simulator comprises of development of a generic structure of Mach Zehnder interferometer and Mach Zehnder delay interferometer that reflect the true photonic operation and not resorting to mathematical representation. In other words, without implicit mathematical derivation of analytical solutions, the MZIM simulator is able to generate various advanced modulation formats including NRZ-ASK, NRZ-PDSK, RZ-ASK, RZ-DPSK with different duty cycles of RZ pulses based on physical biasing voltage and voltage swing of modulating signals. MZDI balanced receiver also exploited physical operating principles to eliminate extensive mathematical simulation to demodulate the received signals. Fiber propagation model using SSF method has been integrated into simulator to evaluate overall system performances with respect to fiber chromatic dispersion and non linearity.

We have demonstrated the optical spectra and eye diagrams of different modulation formats. System performances such as dispersion tolerance of various modulation formats, advantage of balanced detection over single ended detection in DPSK scheme, penalty of mismatch in MZDI have been presented. Analyses of agreements and discrepancies of simulated results with other papers have been discussed in terms of the limitations of the developed models.

The current model of optical transceiver can be developed further by including:

♦ A non perfect optical carrier source to investigate the penalty of spectral width of optical source imposes on various modulation formats and system performances.

♦ Mismatch of two modulating signals in pulse carver in RZ-ASK and RZ-DPSK system that will introduce chirping effect in RZ pulses.

♦ M-ary data encoder to produce multilevel signaling format.

♦ Quantum phase noises in photodiode and EDFA to simulate a linear channel that is dominated by ASE noise. Based on this phenomenon, assumption on Gaussian distributed optical noise is valid to characterize BER of DPSK format using conventional BER method. It is expected that 3 dB advantage of DPSK over ASK could be realized as reported in most of the literature.

♦ Amplitude to phase noise effects

♦ Phase sensitive photonic components, e.g. Raman optical amplifiers, Er doped fibre amplifiers operating in saturation region

♦ Differential phase Q factor calculation taking into account nonlinear transmission penalties of high launch power.

♦ DWDM system to investigate narrow band optical filtering impact on signal bandwidth, ISI penalty and other fiber non linearities such as XPM and FWM.

11   REFERENCES

[1]   A. H. Gnauck and P. J. Winzer, "Optical Phase-Shift-Keyed Transmission," *Journal of Lightwave Technology*, vol. 23, pp. 115-118, January 2005.

[2]   H. Takeshi, O. Vassilieva, Y. Kaori, S. Choudhary, R. Pecqueur, and H. Kuwahara, "Optimal 40 Gb/s modulation Format for Spectrally Efficient Long-Haul DWDM Systems," *Journal of Lightwave Technology*, vol. 20, December 2002.

[3]   W. Xing, L. Xiang, and C. Xu, "Numerical Simulation of the SPM Penalty in a 10 Gb/s RZ-DPSK System," *IEEE Photonics Technology Letters*, vol. 15, pp. 1637, 2003.

[4]   J. C. Palais, *Fiber Optic Communications*, 3rd Ed., Englewood Cliffs, New Jersey: Prentice-Hall, Inc, 1992.

[5]   M. Cvijetic, *Optical Transmission Systems Engineering*. MA: Artech House, INC, 2004.

[6]   K. P. Ho, "Advanced Topics in lightwave Communications Generation of Optical Signals," 2005.

[7]   L. N. Binh and Z. Csematony, "Double Sideband Carrier Suppressed RZ and NRZ modulation format for ultra high capacity 40 Gb/s optical communication system," Monash University MECSE-23, 2003.

[8]   P. J. Winzer, C. Dorrer, R.-J. Essiambre, and I. Kang, "Chirped Return-to-Zero Modulation by Imbalanced Pulse Carver Driving Signals," *IEEE Photonics Technology Letters*, vol. 16, pp. 1379-1381, May 2004.

[9]   K. S. Schneider, "Fiber Optic Communications for the Premises Environment," vol. 2005.

[10]   G. P. Agrawal, *Nonlinear Fiber Optics*. London: Academic Press, InC, 1989.

[11]   G. P. Agrawal, "Fiber Optics Communication System.", J. Wiley 2002.

[12]   D. G. Goff, *Fiber Optic Reference Guide*, Third ed. San Diego: Focal Press, 2000.

[13]   G. P. Agrawal, *Applications of Nonlinear Fiber Optics*. San Diego: Academic Press, 2001.

[14]   J. A. Buck, *Fundamentals of Optical Fibers*, 2nd ed. Hoboken, New Jersey: John Wiley & Sons, Inc, 2004.

[15]   U. Bandelow, A. Demircan, and Martin Kesting, "Simulation of Pulse Propagation in Nonlinear Optical Fibers," Weierstra-Institut fur angewandte Analysis und Stochastik, Berlin ISSN 0946- 8838, 5 May 2003.

[16]   A. F. Elrefaie, R. E. Wagner, D. A. Atlas, and D. G. Daut, "Chromatic Disperision Limitations in Coherent Lightwave Transmission Systems," *Journal of Lightwave Technology*, vol. 6, pp. 704-705, 1988.

[17]   SHF Communication Technologies, "Tutorial note #5 Modulation Schemes." Berlin, Germany.

[18]   C. Xu, X. Liu, and W. Xing, "Differential Phase Shift Keying for high Spectral Efficiency Optical Transmissions," *IEEE Journal of Selected topics in Quantum Electronics*, vol. 10, 2004.

[19]   L. N. Binh and Y. L. Cheung, "DWDM Advanced Optical Communications-SIMULINK models Part 1- Optical Spectra of RZ-NRZ-ASK Modulation Formats,"" Monash University, Melbourne MECSE-3, 2004.

[20]   M. Takeshi, I. Kazuyuki, K. Tatsuya, A. Junichi, k. Kaoru, M. Kuninki, and K. Kumio, "A comparative study of DPSK and ASK WDM Transmission over Transoceanic Distances and Their Performance Degradation due to Non Linear Phase Noise," *Journal of Lightwave Technology*, vol. 21, September 2003.

[21]   C. Xu, X. Liu, L. F. Mollenauer, and X. Wei, "Comparison of Return-to-Zero Differential Phase Shift Keying and On-Off Keying in Long haul Dispersion Managed Transmission," *IEEE Photonics Technology Letters*, vol. 15, Apr 2003.

[22]   Jin Wang and Joseph M. Kahn, "Accurate Bit-Error-Ratio Computation in Nonlinear CRZ-ASK and CRZ-DPSK Systems," *IEEE Photonics Technology Letters*, vol. 16, pp. 2165, 2004.

12   APPENDIX: STRUCTURES OF MACH ZEHNDER MODULATOR
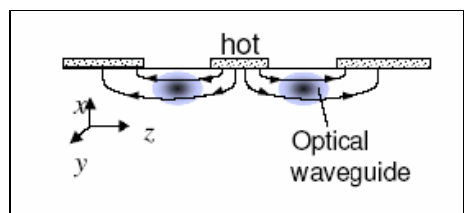
Figure 12- 1 X-cut single drive configuration. [6]

It is clear to show that electric field lines are along z-axis and the electrode of the driving signal is located at either side of the optical waveguide. This configuration is driven by only one electrical drive (data) and it is chirp free due to symmetrical structure that leads to intrinsic balance.
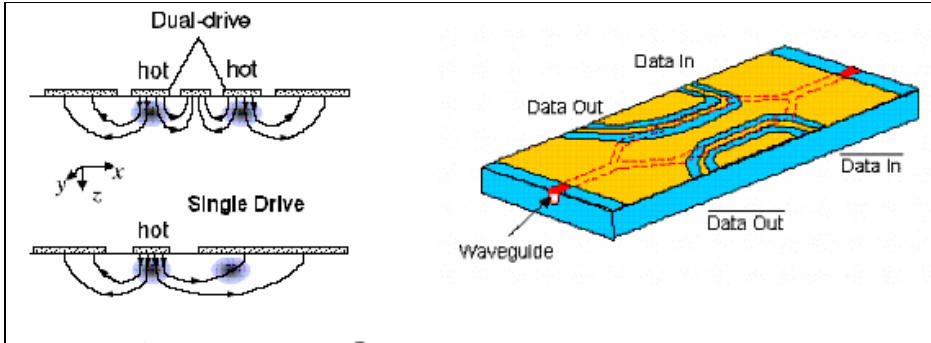
Figure 12- 2 Z-cut single drive and dual drive configuration.[6, 17]

There is a distinct difference from X-cut where electrode of driving signal is located exactly on top of the optical waveguide. Z-cut has better coupling efficiency between electric field ad optical waveguide. Dual drive configuration or push-pull structure employs 2 electrical drives (data and inverted data) to generate modulation. If the electrical field are perfectly matched, i.e. the driving signal amplitude have to be of same amplitude and of opposite phase, the dual drive configuration will be chirp free. Nonetheless, Z-cut single drive configuration has non-zero chirp coefficient because electric field lines pass through 2 optical waveguides are often not similar.[6]

Configuration	Advantage	Disadvantage	Application
♦ Z-cut	♦ - lower and well behaved frequency chirp than EA modulator ♦ - lower V π	♦ -chirped (unchirped only by balanced driving) ♦ - more DC drift than X-cut ♦ Buffer layer required ♦ - single drive not for PSK	♦ Traditionally use for RZ and NRZ (balanced driven)
♦ X-cut	♦ -intrinsically balanced - chirp free ♦ - no need to align the delay (phase) of 2 signals	♦ -electro-optical efficiency lower than Z-cut ♦ Buffer layer required ♦ -higher driving voltage	♦ Suitable for modulation required absolute chirp free
♦ EA modulator	♦ - large linear region	♦ chirp is high and dynamically changing with bias ♦ -high insertion loss ♦ -Modulation <1.0	♦ Cannot be used to PSK

Table 12-1 Summary of advantages, disadvantages and application of X-cut, Z-cut, and EA modulator .